

Review

Mechanism of Iron–Sulfur Cluster Assembly: In the Intimacy of Iron and Sulfur Encounter

Batoul Srour, Sylvain Gervason, Beata Monfort and Benoit D’Autréaux * 

Université Paris-Saclay, CEA, CNRS, Institute for Integrative Biology of the Cell (I2BC), 91198 Gif-sur-Yvette, France; Batoul.srour@i2bc.paris-saclay.fr (B.S.); Sylvain.GERVASON@i2bc.paris-saclay.fr (S.G.); beata.monfort@i2bc.paris-saclay.fr (B.M.)

* Correspondence: benoit.dautreaux@i2bc.paris-saclay.fr

Received: 18 July 2020; Accepted: 30 September 2020; Published: 3 October 2020



Abstract: Iron–sulfur (Fe–S) clusters are protein cofactors of a multitude of enzymes performing essential biological functions. Specialized multi-protein machineries present in all types of organisms support their biosynthesis. These machineries encompass a scaffold protein on which Fe–S clusters are assembled and a cysteine desulfurase that provides sulfur in the form of a persulfide. The sulfide ions are produced by reductive cleavage of the persulfide, which involves specific reductase systems. Several other components are required for Fe–S biosynthesis, including frataxin, a key protein of controversial function and accessory components for insertion of Fe–S clusters in client proteins. Fe–S cluster biosynthesis is thought to rely on concerted and carefully orchestrated processes. However, the elucidation of the mechanisms of their assembly has remained a challenging task due to the biochemical versatility of iron and sulfur and the relative instability of Fe–S clusters. Nonetheless, significant progresses have been achieved in the past years, using biochemical, spectroscopic and structural approaches with reconstituted system *in vitro*. In this paper, we review the most recent advances on the mechanism of assembly for the founding member of the Fe–S cluster family, the [2Fe2S] cluster that is the building block of all other Fe–S clusters. The aim is to provide a survey of the mechanisms of iron and sulfur insertion in the scaffold proteins by examining how these processes are coordinated, how sulfide is produced and how the dinuclear [2Fe2S] cluster is formed, keeping in mind the question of the physiological relevance of the reconstituted systems. We also cover the latest outcomes on the functional role of the controversial frataxin protein in Fe–S cluster biosynthesis.

Keywords: iron; sulfur; iron-sulfur cluster; persulfide; metallocofactor; ISC; SUF; NIF; frataxin; Friedreich’s ataxia

1. Introduction

Iron–sulfur (Fe–S) clusters are small inorganic structures constituting the catalytic site of a multitude of enzymes. They are among the oldest biological cofactors on earth. Their antique role may date back to some four billion years ago, in the form of “Fe(Ni)–S” minerals catalyzing the first abiotic reactions at the origin of life [1–3]. Fe–S clusters then became integral part of living organisms to fulfil a wide range of biochemical reactions [4]. The use of Fe–S clusters by living organisms is now widespread among the prokaryotic, archaeal and eukaryotic worlds [5–9]. Even viruses use Fe–S proteins for their replication [10–12]. With 90 experimentally confirmed Fe–S cluster containing proteins and 60 based on predictions, about 7% of the proteins encoded by the genome of *Escherichia coli* are Fe–S proteins, which emphasizes the prominent roles of Fe–S clusters [13]. Fe–S clusters are composed of iron and sulfide ions, hold in specific protein-binding sites that ligate the iron ions usually via the thiolate of cysteines, but also the nitrogen of histidines and in some rare cases the nitrogen of arginines and oxygen of aspartates or serines [14–17]. The most common forms of Fe–S clusters are the [2Fe2S], [4Fe4S] and

[3Fe4S] clusters which are the building blocks for more complex Fe–S clusters present in enzymes such as nitrogenase, hybrid cluster protein and carbon monoxide dehydrogenase [18–20]. Their biochemical functions can be divided into five main classes: electron transfer, redox catalysis, non-redox catalysis, DNA/RNA binding and maturation of Fe–S cluster proteins [13]. These biochemical functions cover a wide range of biological roles, including ATP production, protein synthesis, oxidative-stress defense and maintenance of genome integrity [7,9,21].

Even though the structures of the elementary Fe–S clusters are relatively simple, these inorganic compounds are not assimilated from the local environment, probably due to their instability. Thereby, the use of Fe–S clusters was concomitant with the development of multi-protein machineries by living organisms to support their biosynthesis [6–9,22]. Four machineries have been identified across species: the NIF (nitrogen fixation), the ISC (iron–sulfur cluster), the SUF (sulfur mobilization) and the CIA (cytosolic iron–sulfur cluster assembly) machineries that each have specialized functions [6–9,22]. In addition, carriers and accessory proteins achieve transport and insertion of Fe–S clusters in dedicated client proteins [6,7]. In eukaryotes, more than 30 proteins are needed to perform their synthesis, transport and insertion [6]. However, only a small subset of these proteins is required for their synthesis, which includes a scaffold protein on which Fe–S clusters are assembled, a cysteine desulfurase providing sulfur in the form of a cysteine bound persulfide (Cys-SSH) and a reductase to reduce the persulfide into sulfide (Figure 1) [23–26]. In a second step, Fe–S clusters are transferred to recipient apo-proteins with assistance of dedicated chaperones and accessory proteins (Figure 1) [6,7,27,28].

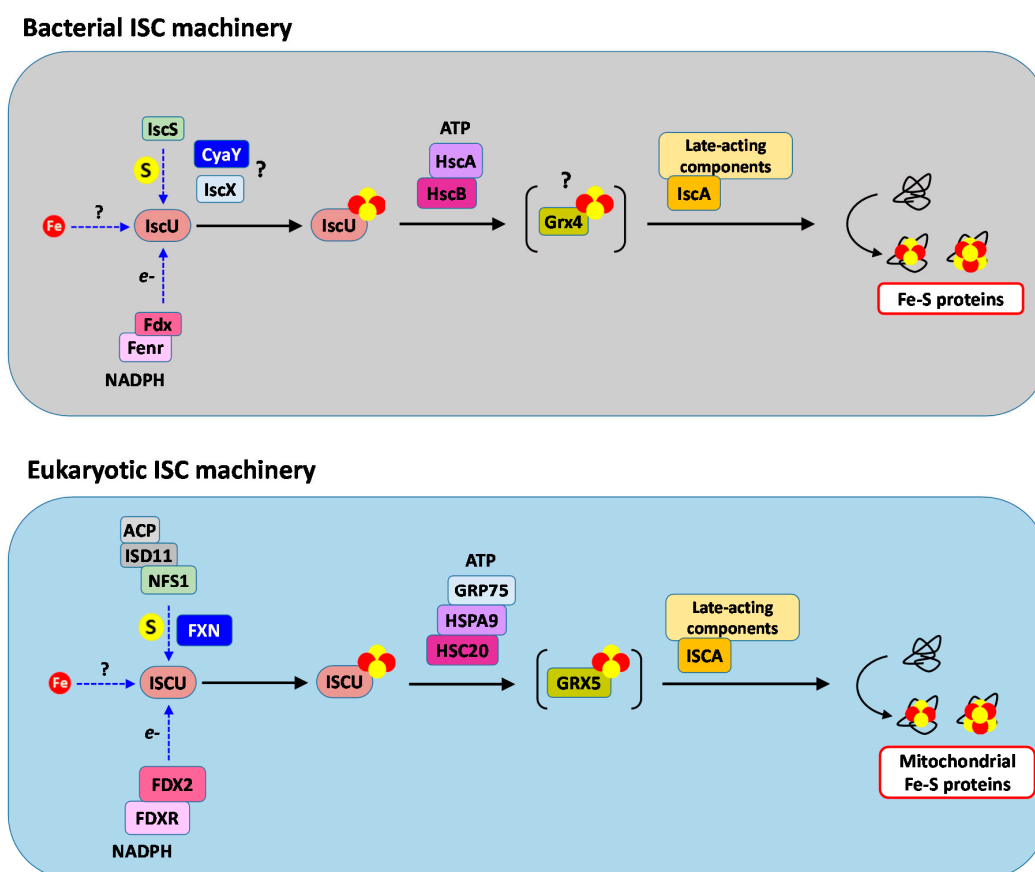


Figure 1. Main components of the bacterial and eukaryotic ISC machineries. The bacterial ISC machinery encompasses proteins encoded by the ISC operon (IscU, IscS, IscX, Fdx, HscA, HscB and IscA), as well

as CyaY, Fenr, Grx4 and several late-acting components. Fe–S clusters are assembled on the IscU scaffold; iron is provided to IscU by a still ill-defined iron chaperone; sulfur is provided by the cysteine desulfurase IscS, and its activity is modulated by CyaY and IscX; and electrons are provided by Fdx that is reduced by the flavodoxin/ferredoxin NADP reductase (Fenr). The [2Fe2S] cluster formed on IscU is transferred to late-acting components by the ATP-dependent chaperone/co-chaperone HscA/HscB. Grx4 may function as a relay to late-acting components among which is the IscA proteins that have specialized functions in the assembly of [4Fe4S] clusters and/or insertion of [2Fe2S] and [4Fe4S] clusters into recipients' enzymes. In the eukaryotic ISC machinery, Fe–S clusters are assembled on the ISCU scaffold, iron is provided to ISCU by a still ill-defined iron chaperone, sulfur is provided by the cysteine desulfurase complex NFS1–ISD11–ACP, and electrons are provided by FDX2 that is reduced by the NADPH-dependent ferredoxin reductase FDXR. Binding of ISD11–ACP to NFS1 maintains NFS1 in a soluble form. FXN stimulates the whole process by acting on the sulfur donation step. The [2Fe2S] cluster formed on ISCU is transferred to late-acting components by the ATP-dependent chaperone/co-chaperone HSPA9/HSC20 with assistance from the nucleotide exchanger GRP75. GRX5 serves as a relay to late-acting components. The late-acting components, including ISCA, have specialized functions in the assembly of [4Fe4S] clusters and insertion of [2Fe2S] and [4Fe4S] clusters into recipients' enzymes. The dashed blue arrows describe the supply of each element needed to build a Fe–S cluster (iron, sulfur and electrons) and the proteins involved at these steps, without assumption on the sequence order and coordination between these singular steps. The solid black arrows describe actual sequence for Fe–S cluster biogenesis and transfer.

Despite huge progresses in the past 30 years to identify all the components of the assembly machineries, a central question remains how Fe–S clusters are assembled. While iron–sulfur clusters can form spontaneously in vitro by mixing iron and sulfide ions in the presence of scaffolding molecules, the biological processes of their synthesis rely on tightly orchestrated reactions to coordinate iron and sulfur insertions in the scaffold proteins. In recent years, combinations of biochemical, spectroscopic, structural and computational approaches with in vitro reconstituted machineries have significantly contributed to the understanding of the mechanism of Fe–S cluster assembly and the specific role of each component of these machineries. Besides, handling these reconstituted systems is a major challenge as reconstituted system can generate free sulfide, which contributes to Fe–S cluster formation in vitro. This process is not expected to be productive of Fe–S clusters in vivo as the sulfide ions can freely diffuse outside of the biosynthetic complexes. Moreover, iron can bind non-specifically to proteins thereby masking specific iron-binding sites. An additional level of complexity arises with the formation of the [4Fe4S] clusters. The current view is that [4Fe4S] clusters are synthesized by reductive coupling of two [2Fe2S] clusters, thus that the [2Fe2S] cluster is the elementary building block of all Fe–S clusters in the cell [6,25,29–33].

This review focuses on the subset of proteins that ensure the biosynthesis of the [2Fe2S] cluster, with a special emphasis on the questions of the synchronization of iron and sulfur supplies to the scaffold proteins, how persulfide is reduced into sulfide and the mechanism of nucleation of iron and sulfide ions leading to formation of the dinuclear [2Fe2S] center. We also review the latest data on the role of the frataxin protein, a key protein in the Fe–S cluster assembly process, the function of which has remained controversial until very recently.

2. Overview of the Fe–S Cluster Assembly Machineries

The NIF system was the first multi-protein machinery to be discovered, in the late 1980s, by Denis Dean's group [34–36]. In nitrogen-fixing bacteria, this machinery is dedicated to the biosynthesis of the M/V and P clusters of the nitrogenase enzyme [18,34–38]. This machinery encompasses two main components, NifU, the scaffold protein and NifS, a cysteine desulfurase that is the source of sulfur [35,36]. Cysteine desulfurases convert the sulfur from the amino acid L-cysteine into a cysteine bound persulfide intermediate (Cys-SSH) that is a source of sulfide ions upon reductive cleavage of its S–S bond. The discovery of cysteine desulfurase was a major advance since this mechanism now

appears as a universal mode of sulfur delivery, not only for Fe–S clusters, but also for the production of a wide variety of sulfur containing biomolecules such as thiolated tRNA, thiamine and Moco [39,40].

In early 1990s, the ISC and SUF machineries were identified as the general providers of Fe–S clusters in most organisms, with the exception of some non-nitrogen fixing bacteria that lack the ISC and SUF machineries, in which the NIF machinery is the general source of Fe–S clusters [5,6,8,9,41–46]. Genome wide analysis show that the occurrence of the SUF system is much higher than the ISC one in bacteria and archaea, thus that the SUF system is the housekeeping assembly machinery in these organisms [47]. In contrast, nearly all eukaryotic organisms rely exclusively on the ISC system that was acquired from bacteria upon endosymbiosis [48], with the exception of plants that rely on both, the ISC and SUF systems [49,50]. In bacteria that encodes both the ISC and SUF machineries, the SUF machinery is expressed under oxidative-stress and iron-deprivation conditions, and in plants, it is expressed in the chloroplast, a compartment that is more exposed to oxidative conditions [8,45]. The underlying reason is that the SUF machinery is more resistant to oxidative stress [51] and handles iron apparently in a more efficient way than the ISC machinery. This raises important questions on the features of the mechanisms of Fe–S cluster assembly that provide such specificities to the ISC and SUF machineries. Some bacteria also express an incomplete machinery, the CSD (cysteine sulfinate desulfinate) system that includes only two components: the cysteine desulfurase CsdA and the sulfur acceptor CsdE that are homologous to the SufS and SufE components of the SUF machinery [9]. The CSD machinery apparently participates to Fe–S cluster biosynthesis by providing sulfur to the SUF machinery [52].

The CIA machinery is present in the cytoplasm of eukaryotic organisms, and in contrast to the other machineries, is not autonomous for sulfur acquisition. Although the cysteine desulfurase of the ISC machinery, NFS1, is also present in the cytoplasm, albeit at very low concentrations, it does not provide sulfur to the CIA machinery [53–56]. Instead, the CIA machinery uses a, as of yet, not identified compound synthesized by the mitochondrial ISC machinery, either a sulfur containing molecule or a preassembled [2Fe2S] cluster [7,25,57]. It is thus unclear whether the CIA machinery is able to synthesize de novo the [2Fe2S] building block. Consequently, we do not cover this topic here.

3. Mechanism of Assembly by the ISC Core Machinery

In bacteria, the genes encoding the components of the machineries are organized in operons. In *E. coli*, the ISC operon encodes eight proteins: **IscU**, the scaffold protein, **IscS**, the cysteine desulfurase, **Fdx**, a [2Fe2S] cluster ferredoxin, **HscA** and **HscB**, a chaperone/co-chaperone system involved in the transfer of Fe–S cluster from IscU to acceptor proteins, **IscA**, a scaffold and/or carrier protein, **IscX**, a putative regulator of the activity of IscS and **IscR** a transcriptional regulator of the whole operon (Figure 1) [22]. Homologs of IscU, IscS, Fdx, IscA, HscA and HscB were later found in yeast, mammals and other organisms with major contributions from Roland Lill's lab to these discoveries (Table 1) [6]. Thereafter, the nomenclature of the protein names of each species is used to describe particular experiments and a double nomenclature bacteria/mammal for more general considerations. Among the proteins of the ISC machinery, **IscS/NFS1**, **IscU/ISCU** and **Fdx/FDX2** together form the core complex for the biosynthesis of [2Fe2S] clusters, while the **IscA/ISCA** proteins have specialized functions in the synthesis of [4Fe4S] clusters from [2Fe2S] clusters and/or transfer of Fe–S clusters (Table 1 and Figure 1) [29–32]. Additional proteins that are not encoded by the ISC operon are needed for the biosynthesis of Fe–S clusters. A flavin-dependent ferredoxin reductase (**Fenr/FDXR**) that uses electrons from NAD(P)H to reduce the [2Fe2S] cluster of Fdx/FDX2 (Table 1 and Figure 1). The frataxin protein (**CyaY/FXN**) is also important for efficient Fe–S cluster synthesis (Table 1, Figure 1) [58,59]. Its exact role is a matter of controversy that we discuss later on [58]. In eukaryotes, **ISD11**, a protein belonging to the LYRM (Leu–Tyr–Arg motif) family, and the acyl carrier proteins (**ACP**) together form a complex with NFS1. The role of the ISD11–ACP complex is incompletely understood, it apparently controls the stability of NFS1 in response to the level of acetyl-CoA [60].

Table 1. Corresponding names of the components of the iron–sulfur cluster (ISC) machinery and accessory proteins in prokaryotes, yeast and mammals.

Functional Role	Prokaryote	Yeast	Mammal
Mitochondrial iron transporter	-	Mrs3/4	MFRN1/2
U-type scaffold	IscU	Isu1/2	ISCU
Cysteine desulfurase	IscS	Nfs1	NFS1
Desulfurase-interacting protein 11	-	Isd11, Lyrm4	ISD11, LYRM4
Acyl carrier protein	ACP	ACP	ACP
Frataxin	CyaY	Yfh1	FXN
IscX	IscX	-	-
Ferredoxin	Fdx	Yah1	FDX2
Ferredoxin reductase	Ferr	Arh1	FDXR
Hsp70 chaperone	HscA	Ssq1	HSPA9
J-type co-chaperone	HscB	Jac1	HSC20
Nucleotide exchanger	-	Mge1	GRPE
Glutaredoxin	Grx4	Grx5	GRX5
A-type scaffold	IscA	Isa1/2	ISCA1/2
Late-acting components	-	Iba57	IBA57
	Bola	Bola1	BOLA1
	-	Bola3	BOLA3
	NfuA	Nfu1	NFU1
	Mrp	Ind1	IND1

3.1. Step 1: Iron Insertion

3.1.1. A Mononuclear Ferrous Iron-Binding Site in IscU/ISCU

IscU/ISCU is a small highly conserved protein of 15 kDa that was identified as the scaffold protein based on its ability to bind a labile [2Fe2S] cluster in vivo when co-expressed with all the other ISC components and in vitro in Fe–S cluster reconstitution assays with IscS/NFS1 [61–63]. Spectroscopic and structural studies of bacterial, archaeal and eukaryotic IscU/ISCU proteins have provided evidence that the [2Fe2S] cluster is ligated in an asymmetric arrangement by well-conserved amino acids: three cysteines and a non-cysteinylligand most likely an aspartate [23,61,62,64–66]. This assembly site was thus proposed to be the entry point for iron.

However, metal titrations and tri-dimensional structures revealed that IscU/ISCU proteins purified from bacterial cells do not contain iron in the assembly site but a zinc ion instead [23,67–72]. The zinc ion was found coordinated in an overall tetrahedral geometry by the well-conserved amino acids of the assembly site in *Haemophilus influenza* [71] and *Mus musculus* (PDB code 1WFZ) IscU and the identity of the ligands was also assessed in *E. coli*, mouse and human IscU/ISCU using site directed mutagenesis experiments (Figure 2A) [23,68,69] Here and thereafter, to ease comparison, the mouse sequence is used for amino acid numbering in IscU/ISCU proteins. In these proteins, the Zn²⁺ ion is coordinated by the two cysteines Cys35 and Cys61 that are also ligands of the [2Fe2S] cluster, and the histidine His103, but the fourth ligand seems exchangeable. While the aspartate Asp37 is the fourth ligand in the vast majority of cases, it is exchanged by the cysteine Cys104 in the crystal structure of IscU from *H. influenza* [71]. This suggests structural plasticity of the metal-binding site. Analysis by quantum and molecular mechanics indeed indicate that small rearrangements, such as protonation of the ligands, could induce a ligand swapping at the zinc site [69]. This structural plasticity would facilitate the accommodation of several metal and sulfide ions.

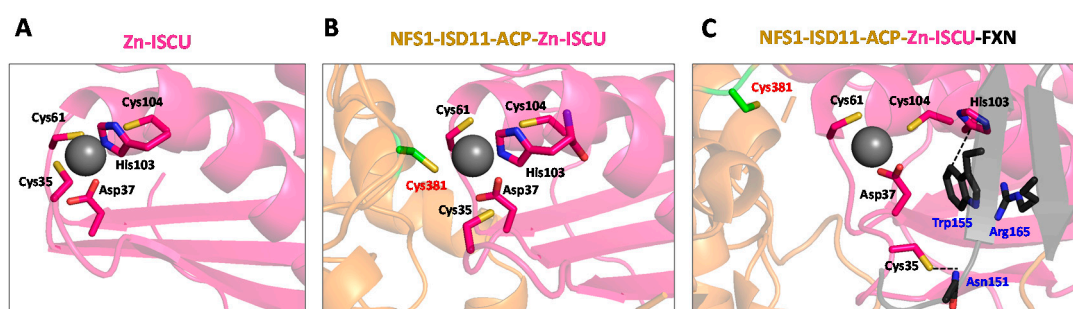


Figure 2. Structural rearrangement at the zinc site of ISCU upon binding of NFS1 and FXN. Zoom on the zinc site of (A) mouse ISCU (nuclear magnetic resonance (NMR) structure, PDB code 1WFZ) and in the human NFS1–ISD11–ACP–ISCU complex (B) without FXN (X-ray structure PDB code 5WLW) [67] and (C) with FXN (CryoEM structure PDB code 6NZU) [73]. ISCU and some of its key amino acids (Cys35, Asp37, Cys61 and His 103) are colored in pink, NFS1 is in yellow with its catalytic cysteine (Cys381) in green and FXN with its key amino acids (Asn151, Trp155 and Arg165) are in black. The dashed black line represents π staking between Trp155 and His103. The zinc ion is initially coordinated by Cys35, Asp37, Cys61 and His103 in ISCU. Upon binding to NFS1, the catalytic cysteine of NFS1, Cys381, binds to the zinc ion via exchange with Cys35. FXN binds to the NFS1–ISD11–ACP–ISCU complex and pushes aside His103 and Cys35 of ISCU via interactions with Trp155 and Asn151, respectively, thereby uncovering Cys104.

The plasticity of the IscU/ISCU protein also prevails at the level of its ternary structure and is directly connected to the metal-binding site. NMR studies revealed that IscU/ISCU exists in two inter-converting forms, a structured one and a de-structured one [69–71,74–76]. Interestingly, the coordination of the metal ion stabilizes the structured form. The ligands of the zinc ion belong to different parts of the protein: the cysteine Cys35 and the aspartate Asp37 are carried by a linker between two β -sheets, the cysteine Cys61 is at the tip of an α -helix and the histidine His103 along with the cysteine Cys104 are at the tip of another α -helix. Therefore, the coordination of the zinc ion connects distinct parts of the protein which stabilizes the ternary structure of the protein.

The first evidence suggesting that iron binds in the assembly site came from an NMR study on the *E. coli* IscU protein, which reported that incubation of apo-IscU with iron stabilizes the ordered form, as observed with zinc [77]. Our lab recently conducted an extensive study on mouse ISCU using several spectroscopic methods [23]. We found that the zinc ion hinders iron binding in the assembly site, but upon removal of the zinc ion, the monomeric form of ISCU binds Fe^{2+} in the assembly site. Site-directed mutagenesis identified Cys35, Asp37, Cys61 and His103 as the ligands of the iron center [23]. The Fe^{2+} ion thus adopts a similar arrangement as the Zn^{2+} ion in the assembly site of ISCU, which suggests interchangeable roles. Titration by circular dichroism (CD) indicated that ISCU binds a single Fe^{2+} ion and Mössbauer spectroscopies showed that it is a high spin $\text{Fe}(\text{II})$ center and confirmed the presence of several cysteines in the coordination sphere of the metal. Fe–S cluster assembly assays using the complete mouse ISC machinery with the NFS1–ISD11–ACP complex, FDX2 and FDXR show that iron-loaded ISCU (Fe –ISCU) is competent for Fe–S cluster assembly, while the zinc-loaded form (Zn –ISCU) is not, which indicates that binding of iron in the assembly site is the initial step in Fe–S cluster biosynthesis [23]. Binding of iron in the assembly site was later on reported with *E. coli* IscU upon removal of the zinc ion, which suggests that the first step in the mechanism of Fe–S cluster synthesis is conserved [78].

Surprisingly, the investigations of iron-binding sites in IscU/ISCU proteins from *E. coli*, human, drosophila and yeast by X-ray absorption spectroscopy (XAS) led to the conclusion that iron does not initially bind in the assembly site but in a 6-coordinated site comprising only nitrogen and oxygen [79–81]. A similar species was detected by Mössbauer spectroscopy when mouse apo-ISCU was incubated with one equivalent of iron, but this species represents a minor fraction of iron (15%) [23]. Experiments conducted with sub-stoichiometric amounts of iron showed that only the assembly site is

filled, thus that iron has a poor affinity for the putative secondary site. Moreover, reconstitution assays with ISCU containing iron exclusively in the assembly site showed that it is still fully competent for Fe–S cluster assembly, which rules out the idea that the minor fraction is important for Fe–S clusters synthesis, thus that there is a defined secondary site in ISCU [23]. This species most likely represents iron bound non-specifically to the protein. It must be noted that mouse ISCU is a difficult protein to handle as the disordered form that accumulates in the absence of metal forms higher order oligomers that do not bind iron. Thereby, the discrepancy with the XAS data may relate to protein preparations and buffer conditions if the other IscU/ISCU proteins behave similarly to mouse ISCU.

3.1.2. Iron Donor to IscU/ISCU

The fact that IscU/ISCU contains a zinc ion that hinders iron binding raises the question of the physiological mechanism of iron insertion. In vivo, the presence of the zinc might prevent accumulation of the disordered form. However, since zinc has a higher affinity than iron for IscU/ISCU [23,69], a still ill-defined metallochaperone might be required to exchange the metals. These data also raise the question of the physiological iron donor to IscU/ISCU.

Frataxin

The frataxin protein was initially proposed to function as an iron storage/donor for IscU/ISCU [82–87]. Although the iron-storage/chaperone function has been questioned by several studies [58], and the most recent data indicate that frataxin is an accelerator of persulfide transfer (see Section 3.5) [23,88,89], the iron chaperone hypothesis is still favored by a number of groups [90–96].

Eukaryotic cells that are defective or deleted for the gene encoding the frataxin protein display growth phenotypes associated with a deficit in Fe–S cluster biogenesis [97–101]. Indeed, the bacterial and eukaryotic frataxins interact with the core IscS–IscU and NFS1–ISCU complexes of the ISC machinery, indicating a direct role in Fe–S cluster biogenesis [86,102–105]. In humans, inherited mutations in the non-coding sequence of the frataxin locus lead to Friedreich’s ataxia (FA), a neurodegenerative and cardiac disease [106]. This discovery has strongly fostered the research in the past years to elucidate the function of frataxin.

Based on the observations that (i) frataxin deficient cells accumulate iron in mitochondria and that (ii) bacterial CyaY and yeast Yfh1 frataxins bind ferric iron, which triggers auto-assembly into multimers, the hypothesis that frataxin functions as an iron storage has emerged [58,82,83,85,97,99,107,108]. However, the iron-storage function was challenged by several other studies. First, human frataxin (FXN) self-assembles into oligomers only under extreme conditions and in an iron-independent manner [109]. In yeast and mouse fibroblast, the self-assembly of frataxin is dispensable for its physiological function [110,111]. In yeast, overexpression of Yfh1 is unable to mitigate iron accumulation and binding of iron to Yfh1 could not be confirmed by immunoprecipitation [112,113]. In bacteria, the function of CyaY appears restricted to iron-rich conditions. Although this may be consistent with a role in iron storage, in yeast, there is no obvious effect of iron on the phenotype of cells lacking Yfh1 [59,97]. In mammals, a cardiac mouse model of FA showed that the accumulation of iron is not a primary defect but rather a consequence of the Fe–S cluster deficit [100]. Finally, the accumulation of iron is not a specific feature of frataxin deficiency since any defect in one of the core components of the ISC machinery also leads to dysregulated iron metabolism [114]. Altogether, these data have disqualified the iron-storage function for frataxin.

The frataxin protein was also proposed to function as an iron chaperone for IscU/ISCU, since monomeric frataxin from various organisms bind iron in vitro and several reconstitutions suggested that frataxin brings iron to the ISC machinery [86,87,92]. However, the number of iron-binding sites in frataxin varied from one study to another (from one to seven iron-binding sites), with both Fe²⁺ and Fe³⁺ binding with similar affinities, which rather suggest non-specific iron binding [82,87,108,115–118]. Indeed, FXN lacks a defined metal-binding site associated with well-conserved ligands such as cysteine, histidine and aspartate, but contains an acidic region that

binds several metals non-specifically via electrostatic interactions. This may provide a mean for frataxin to bring several labile iron ions nearby the assembly site of IscU/ISCU, but with low specificity, which is difficult to rationalize with a specific role in iron donation. Moreover, data from our group indicated that mammalian FXN is not required for iron insertion in ISCU [23]. Altogether, these data argue against a role of frataxin in iron donation; instead, a function as an accelerator of persulfide transfer is now proposed (see Section 3.5).

ISCA

A-type proteins (IscA, NiflscA and SufA) from various organisms were shown to bind ferric iron with high affinity and to provide iron to IscU/ISCU in Fe–S cluster reconstitution assays through a cysteine mediated process [119–125]. The Fe(III) center of bacterial IscA can be reduced by L-cysteine and released as free or cysteine bound Fe²⁺ ions, which provide a source of iron for IscU [119,125]. However, several *in vivo* studies argue against a role of the IscA/ISCA proteins in iron donation. First, deletion of the genes encoding the Isa1 and Isa2 proteins in yeast led to a slight increase in the iron content of Isu1, instead of lowering it as expected for an iron chaperone [32]. Several groups found that A-type proteins do not co-purify with iron alone but with a Fe–S cluster [126–129]. Indeed, *in vivo* and *in vitro* data rather point to a role of the A-type proteins as scaffolds for the synthesis of [4Fe4S] clusters or in the transfer of [2Fe2S] and [4Fe4S] clusters [29,32,126,127,129,130]. Moreover, while no interaction with IscU/ISCU has been reported so far, the IscA/ISCA proteins interact with the late-acting components of the Fe–S cluster biogenesis pathway, which strengthen the idea that they are not involved at the early steps, i.e. iron insertion [29,131–133].

Connection with the Labile Iron Pool

If not frataxin or IscA/ISCA, then how does IscU/ISCU acquire iron? Only few iron metallochaperones have been identified in eukaryotes and prokaryotes [134–137]. Ferrochelatase is possibly the only attested iron chaperone in mitochondria [134]. Indeed, a general view of iron speciation in proteins is that non-heme iron proteins acquire their metal from a labile iron pool [135–137]. Due to the low structural diversity of metal-binding sites in proteins to discriminate one metal from another, insertion of the proper metal is controlled by its bioavailability and its intrinsic affinity, which follows the Irving–Williams series [135–137]. Thereby, metals with intrinsic high affinity are kept at very low concentration while weaker binders are present in the form of labile pools. Iron is among the weaker binders and the existence of labile iron pools is now corroborated by several studies. Recent investigations of cellular iron contents by Mössbauer spectroscopy suggest that it is composed of non-heme high-spin Fe(II) complex with primarily O and N donor ligands in concentrations estimated in the range of 1 to 10 µM, which is very close to the affinity of iron for most proteins [135–142]. Low-molecular-weight iron complexes with a mass-range of 500 to 1300 Da have been isolated from bacteria and mitochondria that may be central components of this labile iron pool [139–142]. Iron delivery to protein from these labile iron pools may involve small molecules, such as glutathione (GSH), instead of metallochaperones [137,143]. Finally, even though a chaperone is possibly dispensable for iron insertion, the most important step could be the release of the zinc ion from IscU/ISCU, which would require a chelatase.

3.2. Step 2: Sulfur Insertion

3.2.1. Two Different Classes of Cysteine Desulfurase

The second key step of Fe–S cluster synthesis is the insertion of sulfur. The cysteine desulfurases IscS and NFS1 are the source of sulfur for Fe–S cluster assembly in the ISC machinery. Cysteine desulfurases provide sulfur in the form of a persulfide bound to their catalytic cysteine (Cys-SSH) [39]. This persulfide is produced by desulfurization of L-cysteine catalyzed by their cofactor, a pyridoxal phosphate (PLP), which leads to formation of a persulfide on their catalytic cysteine. PLP-dependent enzymes form

a huge family that perform various types of elimination and substitution reactions on amino acids and their derivatives. Several structures of cysteine desulfurase have been solved and all revealed an arrangement as homodimers, in which the PLP-binding pocket of one subunit is completed by the second one (Figure 3A,B) [39,67,144–150]. Cysteine desulfurases also display key differences allowing their categorization in two classes owing to the length of the mobile loop carrying their catalytic cysteine [39]. This loop is much longer in class I than in class II enzymes, which facilitates long-range sulfur delivery to acceptors for class I enzymes. IscS and NFS1 as well as NifS belong to class I, while SufS, the cysteine desulfurase of the SUF machinery, belongs to class II.

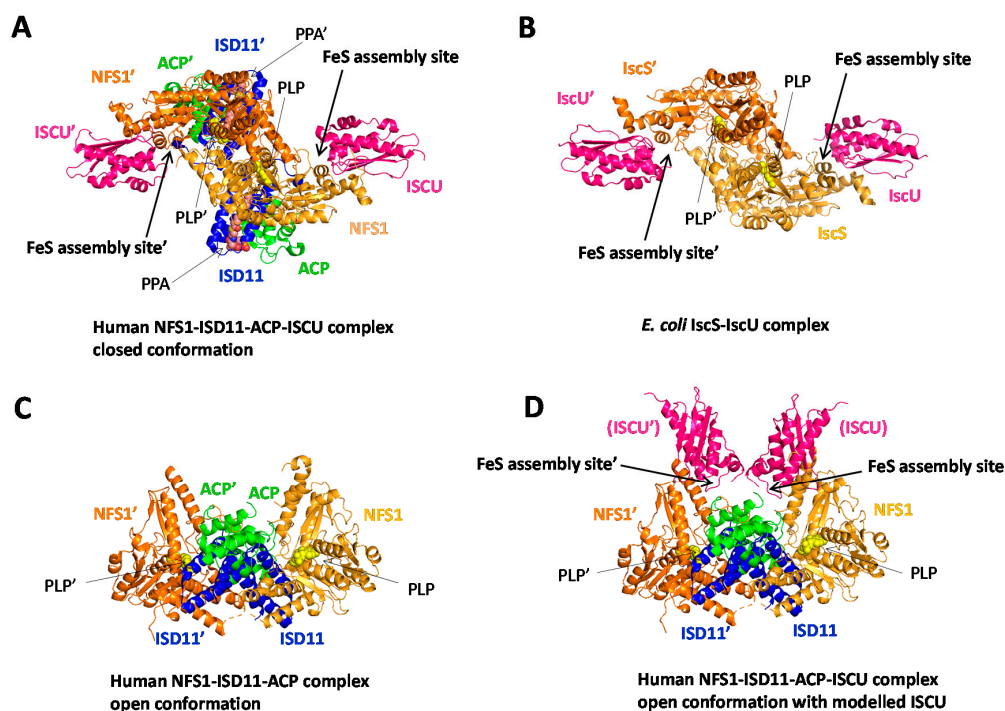


Figure 3. Structures of the human NFS1-ISCU and *E. coli* IscS-IscU complexes. X-ray structures of (A) human NFS1-ISCU complex in the closed conformation (PDB code 5WLW) [67], (B) *E. coli* IscS-IscU complex (PDB code 3LVL) [150], (C) human NFS1-ISCU complex in the open conformation (PDB code 5USR) [151] and (D) human NFS1-ISCU complex in the open conformation (PDB code 5USR) with the human ISCU proteins modeled according to the structure of the NFS1-ISCU complex (PDB code 5WLW). The labels for the ACP protein have been omitted for clarity in D. IscS/NFS1 are colored in orange, IscU/ISCU in pink, ISD11 in blue and ACP in green. The pyridoxal phosphate (PLP)-binding sites, the phosphopantetheine with its fatty acyl chain (PPA) and the Fe-S cluster assembly sites of IscU/ISCU are indicated by arrows.

Moreover, in eukaryotes, NFS1 forms a tight complex with the ISD11-ACP complex that regulates the activity of the ISC system in response to the level of acetyl-coA [60,67,151]. The crystal structure of the human NFS1-ISCU complex shows that binding of ISD11-ACP to NFS1 is mediated by ISD11 and that ACP is anchored to ISD11 via its fatty acid chain (Figure 3A) [67]. The ISD11-ACP complex stabilizes NFS1 since in its absence, NFS1 is poorly soluble [152,153]. The crystal structure of the complex indeed shows that ISD11 binds to a hydrophobic patch composed of Leu78 and Ile82 at the surface of NFS1, which most likely helps maintain NFS1 in a soluble form [67].

Strikingly, another crystal structure of the human NFS1-ISCU complex was solved which displays a completely different arrangement of the NFS1 and ISD11 proteins relative to each other while keeping the overall structure of the ISD11-ACP complex (Figure 3C) [67,151]. In this structure, the dimer interface is created by contacts between the hydrophobic patch of each NFS1 and via ISD11 that connects the two subunits of NFS1. The PLP-binding pocket is incomplete and thus the protein is

most likely catalytically inactive. This conformation is designated as open conformation [151] and the conformation in which the PLP-binding pocket is complete, is called the closed conformation [67]. It is still unclear whether the open conformation has a physiological relevance.

3.2.2. Mechanism Generating Persulfide in Class I Cysteine Desulfurase

While the mechanism of sulfur delivery clearly differentiates class I and II cysteine desulfurase, the mechanism of desulfurization is similar for both enzymes [39]. This mechanism relies on catalysis by the PLP cofactor which operates as an electron withdrawal group facilitating the elimination of sulfur on L-cysteine (Figure 4). The PLP cofactor is anchored to the enzyme via the side chain of a lysine through formation of an imine link, also called internal aldimine. The amino group of the L-cysteine substrate binds to the PLP by exchange with the amine of the lysine to form an external aldimine. This intermediate is converted into a ketimine in which a double bond is created between the enantiomeric α carbon of L-cysteine and its amino group. Then, the sulfur of L-cysteine is eliminated and “transferred” to the catalytic cysteine of the cysteine desulfurase, which leads to formation of a persulfide (-SSH) and creation of a double bond between the α and β carbon of the L-cysteine. Upon hydrolysis, alanine is released and a new cycle is initiated. Formally, a sulfanium cation (HS^+) is abstracted by the thiolate group of the catalytic cysteine. This formal description suggests that the reaction is an oxido-reduction process. The redox state of the terminal sulfur (also called sulfane sulfur) is commonly assumed to be “0” while the sulfur of the cysteine to which it is bound would stay at the -II redox state. However, this description is not correct since two identical atoms that are covalently attached have their redox state mutually affected and equals, as found in disulfides (RSSR') and hydroperoxides (ROOH) in which the sulfur and oxygen atoms are at the same -I redox state. Thereby, the formal redox states of the sulfurs in a persulfide are better described as -I for both of them, which indicates that the sulfur of L-cysteine is oxidized during the reaction and consequently the carbon carrying the sulfur of L-cysteine is reduced from -I to -III in L-alanine (Figure 4, red labels).

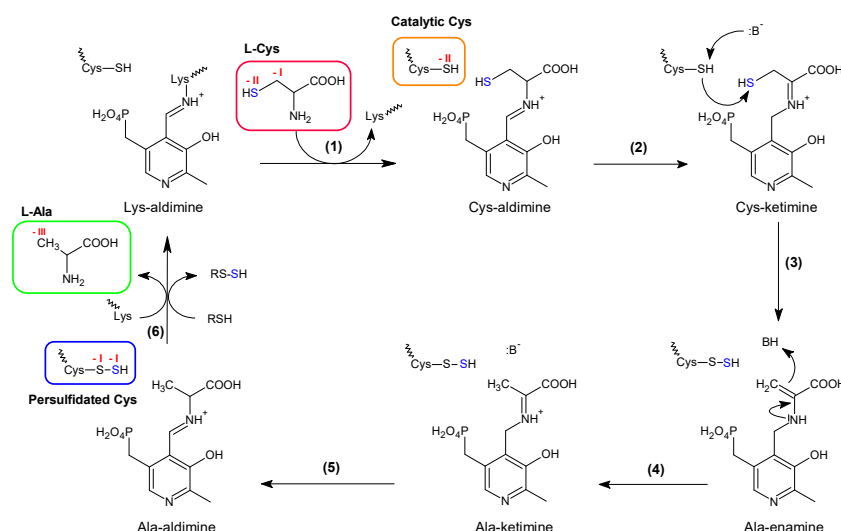


Figure 4. Mechanism of persulfide formation by cysteine desulfurases. The scheme presents the main intermediates in the catalytic cycle of cysteine desulfurases. The PLP cofactor is bound to the cysteine desulfurase backbone via the nitrogen of a lysine residue, in the form of a Lys-aldimine. The L-cysteine substrate exchanges with the lysine to form a Cys-aldimine (1), which is rearranged into a Cys-ketimine (2). A base ($:\text{B}^-$) deprotonates the thiol of the catalytic cysteine of the cysteine desulfurase and the resulting thiolate reacts with the thiol of the Cys-ketimine intermediate, which leads to formation of a persulfide on the catalytic cysteine (3). Concomitantly, a double bond is created with the carbon of the former L-cysteine substrate in the form of an Ala-enamine (3). Upon protonation, the Ala-enamine is converted into Ala-ketimine (4) and then Ala-aldimine (5). The sulfane sulfur (blue) of the persulfide is transferred to a thiol acceptor and L-alanine is released by exchange with the internal lysine residue (6).

The formal oxidation states of the relevant atoms of the reaction (sulfur and adjacent carbons) are indicated in red for the starting and final material. The reaction starts with two sulfurs at the -II oxidation state in L-cysteine and the catalytic cysteine with a carbon at -I in L-cysteine to end up with two sulfurs at the -I oxidation state in the persulfidated catalytic cysteine and a carbon at -III in L-alanine.

3.2.3. Sulfur Transfer to the IscU/ISCU Scaffold, a Metal-Driven Process

The first studies on the process of sulfur supply to IscU/ISCU were reported almost 20 years ago, with *A. Vinelandii* and *E. coli* IscS and IscU [154–156]. These studies showed that IscS transfers several persulfides to IscU. A sulfur-first model was then proposed, in which the persulfides are transferred and later on reduced upon binding of Fe^{2+} ions. Surprisingly, several persulfides (2 to 4) accumulated on IscU, which was difficult to rationalize with the requirement of only two sulfurs for the formation of a $[\text{2Fe2S}]$ cluster [154,156]. Another study with *T. maritima* IscU mentioned that the persulfides transferred to IscU were not reducible by iron, unless iron was already bound to IscU prior to persulfide transfer [157]. Although the experimental data were not shown, an iron-first model was proposed, in which the iron binds first then a persulfide is transferred and reduced by iron. Thereby, controversies on the number of persulfide transferred to IscU/ISCU and the sequence of iron and sulfur insertions have emerged with two opposite models: sulfur-first and iron-first. It is now becoming clear that iron comes first and triggers the transfer of a persulfide (Figure 5) [23,89].

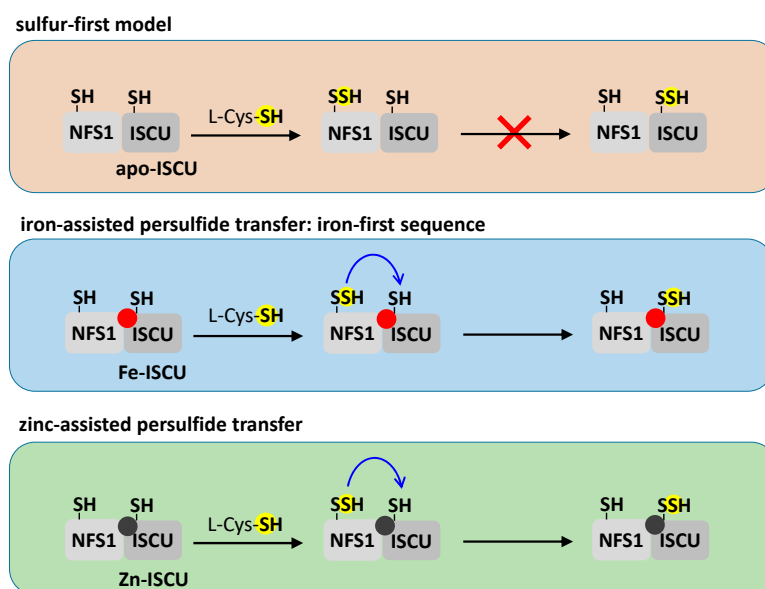


Figure 5. Metal-dependent persulfide transfer in the NFS1–ISCU complex. The sequence corresponding to the sulfur-first and iron-first models are depicted in the top two panels. First, a persulfide is formed on the catalytic cysteine of NFS1 (Cys381). Then, in the absence of a metal in ISCU (apo-ISCU), the persulfide of NFS1 is not transferred to ISCU (as shown by the red cross), which invalidates the sulfur-first model. In the presence of iron (red sphere, Fe–ISCU), the persulfide of NFS1 is transferred to the cysteine Cys104 of ISCU, which highlights the iron-first model. The third panel shows that, when zinc (dark gray sphere, Zn–ISCU) is present in the assembly site, instead of iron, it also triggers persulfide transfer. The blue arrows refer to movement of sulfur in trans-persulfuration reactions.

Persulfide transfer was also reported with the mouse and human NFS1–ISD11–ACP–ISCU complex [88,158]. Our analysis using mass spectrometry and an alkylation assay developed to directly visualize and quantify protein-bound persulfides, has established that a single persulfide is transferred to mouse ISCU [88]. The cysteine Cys104 was identified by mass spectrometry as the final persulfide receptor [88]. Furthermore, the transfer of persulfide to ISCU was correlated with Fe–S cluster assembly

thus indicating that it is a relevant step in this process (see next section) [23]. The accumulation of more than one persulfide was also observed with the mouse system but at longer time course and was not correlated with Fe–S cluster assembly, which may explain the transfer of multiple persulfides previously observed with *A. Vinelandii* and *E. coli* IscU proteins [23,88].

Interestingly, with the mouse system it was shown that in the absence of iron, the transfer of persulfide is abolished, which points to a metal-dependent process [23]. A similar iron-dependent persulfide transfer process was recently reported with the *E. coli* system [78]. Thus, the presence of iron is required to allow the transfer of persulfide, which experimentally confirms the iron-first model that was earlier proposed and discards the sulfur-first hypothesis (Figure 5). Surprisingly, persulfide transfer to ISCU is also enabled when zinc is in the assembly site, which is probably related to the identical coordination mode of iron and zinc in ISCU (Figure 5). This may indicate a physiological role for zinc as proposed for the zinc ion of SufU, a closely related homolog of IscU/ISCU (see Section 5.3.3) [159]. Moreover, the iron-like effect of zinc may explain the initial controversy in the models of iron and sulfur insertion sequences. Since zinc was likely present in the preparations of IscU, although its presence was not assessed [154–156], it has probably allowed persulfide transfer in the absence of iron and misled the authors to the conclusion that sulfur comes first.

Trans-persulfuration reactions are common to several sulfur insertion processes but none of them have been described as iron-dependent [39,40]. Indeed, this feature is likely specific to Fe–S cluster assembly systems as it coordinates sulfur supply with the presence of iron in ISCU. This raises the question of the mechanism of this new type of reaction. Since both, iron and zinc, enable persulfide transfer, the examination of the structures of the NFS1–ISCU complexes solved with zinc may help elucidate this mechanism. The X-ray structure of the human NFS1–ISD11–ACP–ISCU complex shows that the catalytic cysteine of NFS1 binds to the zinc center through exchange with Cys35 of ISCU (Figure 2B) [67]. Thus, the metal ion may play a structural role by positioning the catalytic cysteine of NFS1 at a short distance of the receptor cysteine (Cys104) of ISCU and additionally may play the role of a Lewis acid catalyst by providing an electrophilic character to the sulfane sulfur of the persulfide to promote the nucleophilic attack by the receptor cysteine on the persulfide. However, Cys104 is shielded by the metal ion and its surrounding ligands (Asp37, Cys61 and His103), which seems to preclude a direct transfer of persulfide to this residue. Persulfide transfer could thus be indirect via Cys35 or Cys61 as relays. However, a mutation of the cysteine Cys104 to serine does not lead to accumulation of a persulfide on Cys35 or Cys61 as expected if they were functioning as relays, which tends to invalidate this hypothesis [23,88]. Therefore, in keeping with the structural plasticity of ISCU discussed in the previous section, a structural rearrangement uncovering Cys104 to facilitate persulfide transfer seems more likely.

In conclusion, the detailed study of the persulfide transfer process provides the first compelling evidence of an iron-first mechanism in which persulfide transfer is triggered by the presence of iron in IscU/ISCU [23,78]. This represents the first encounter of sulfur with iron in the Fe–S cluster assembly process.

3.3. Step 3: Persulfide Reduction

3.3.1. Reduction by Iron

To generate the sulfide ions that are the constituents of Fe–S clusters, the persulfide must be reduced into sulfide. As discussed in the previous section, Fe²⁺ ions were initially proposed to be the reductant of the persulfide thereby yielding Fe³⁺ and sulfide ions, to generate an oxidized [2Fe2S]²⁺ cluster [154,155,157]. However, no reduction was observed with the mouse system after transfer of persulfide to ferrous iron-loaded ISCU [23]. Furthermore, the reduction of a persulfide by Fe²⁺ is chemically irrelevant since this reaction requires two electrons and Fe²⁺ provides only one electron by switching to the Fe³⁺ state.

3.3.2. Reduction by Thiols

Thiols, essentially dithiothreitol (DTT), but also GSH and cysteine were extensively used as reductants in Fe–S cluster reconstitution studies [61,78,158,160–164]. However, their mode of action was not thoroughly investigated until recently. Using the mouse ISC system, our group reported that thiols are able to release sulfide by direct reduction of the persulfide of NFS1, but are poorly efficient to reduce the persulfide transferred to ISCU, probably due to the presence of the metal that shields the receptor cysteine Cys104 [88]. The reduction of the persulfide of NFS1 by thiols occurs in reaction performed with excess of L-cysteine relative to the NFS1–ISCU complex (Figure 6A). Under these conditions, a persulfide is formed on NFS1 that is transferred to ISCU, then a new persulfide is formed on NFS1 that cannot be transferred to ISCU since it is already persulfidated, which leads to a complex persulfidated on both, NFS1 and ISCU. Since thiols react faster with NFS1 than with ISCU, this leads to preferential reduction of the persulfide sitting on NFS1. Thereby, the prominent source of sulfide ions in thiol-based reconstitution is NFS1 not ISCU. This reduction proceeds in two steps: (1) trans-persulfuration of the thiol leading to a persulfidated thiol (RSSH) and (2) cleavage of the S–S bond of the persulfidated thiol by another thiol molecule (Figure 6A). The sulfide ion then combined with iron to form a Fe–S cluster. The thiol-based reactions indiscriminately lead to formation of both [2Fe2S] and [4Fe4S] clusters with variable proportions [61,162,164–167]. DTT further enhances the proportion of [4Fe4S] cluster versus [2Fe2S] and also generates high-molecular-weight (HMW) Fe–S minerals [167]. This was attributed to the ability of DTT to stimulate the rate of sulfide release more strongly than L-cysteine, thereby creating a bulk of sulfide that reacts with [2Fe2S] clusters to generate [4Fe4S] clusters and eventually forms HMW Fe–S minerals. Surprisingly, the thiol-based reconstitution is also operative when zinc is present in the assembly site of ISCU, but is much slower probably due to hindrance of Fe–S cluster formation by the zinc ion [23].

Such thiol-based Fe–S cluster assembly reactions rely on “free” sulfide ions and their production is not coupled with the presence of iron. This type of reaction is probably inefficient *in vivo* for Fe–S cluster assembly as the sulfide ions will diffuse outside of the ISC complex and the probability of iron and sulfur encounter will be very low. Therefore, thiol-based reactions are not considered as physiologically relevant for Fe–S cluster assembly.

3.3.3. Ferredoxin and Iron Mediated Reduction of Persulfides

The [2Fe2S] ferredoxin Fdx/FDX2 was also proposed to function as a reductant of persulfides. The deletion of the gene encoding Fdx in *E. coli* and the depletion of Yah1 in the yeast *Saccharomyces cerevisiae*, both led to impaired Fe–S cluster biosynthesis [168–171]. Moreover, *yah1* is an essential gene in yeast, which points to a critical role of ferredoxins [169]. In human, two ferredoxins are present in mitochondria, the adrenodoxin (FDX1), and a closely related homolog named FDX2 (or FDX1-like) [172]. FDX1 is mainly expressed in adrenal glands where it is involved in steroid biosynthesis, while FDX2 is ubiquitously expressed and is essential for Fe–S cluster biogenesis in mitochondria [172]. Another study reported that both FDX1 and FDX2 function in Fe–S cluster biosynthesis [173]. However, the tissue specificity of FDX1 to adrenal glands most likely dictates its role. Cognate reductase partners were identified in *E. coli* (the ferredoxin–NADP reductase FerR), human (FdxR) and yeast (adrenodoxin reductase Arh1) that provides electrons from NAD(P)H to Fdx/FDX2 (Table 1) [169,173–175].

Fe–S cluster reconstitution assays showed that *E. coli*, yeast and mouse ferredoxin/ferredoxin reductase systems are able to replace DTT [23,24,176]. NMR studies with mouse and bacterial proteins reported that Fdx binds IscS [177–179]. It was thus proposed that Fdx reduces the persulfide of IscS into sulfide. However, this mechanism is reminiscent of the thiol-based reconstitution in which sulfide is released irrespective of the presence of iron. Moreover, IscU was reported to displace Fdx, thereby preventing synchronization of sulfide production with the presence of IscU to uptake these sulfide ions [178]. In contrast, NMR and SAXS studies of the eukaryotic *Chaetomium thermophilum* ISC complex showed that FDX interacts with both NFS1 and ISCU [24,67]. The first experiments

directly testing the effect of ferredoxin on the persulfide of NFS1 and ISCU were carried out with the mouse system by tracking the persulfide during the reaction, using mass spectrometry and alkylation assays [23]. The step-by-step analysis revealed that FDX2 selectively reduces the persulfide transferred to Fe-ISCU but does not reduce the persulfide of NFS1 (Figure 6B). Importantly, this reduction step leads to formation of a [2Fe2S] cluster in ISCU, thus indicating that it is a critical step of the assembly process. Titrations have further indicated that this reaction is highly efficient with about 90% of L-cysteine converted into a [2Fe2S] cluster whereas thiol-based reactions are poorly efficient with only 5% of L-cysteine actually incorporated as sulfide ions in the Fe-S cluster. Moreover, the FDX2-based reaction is about 100 times faster than the thiol-based one.

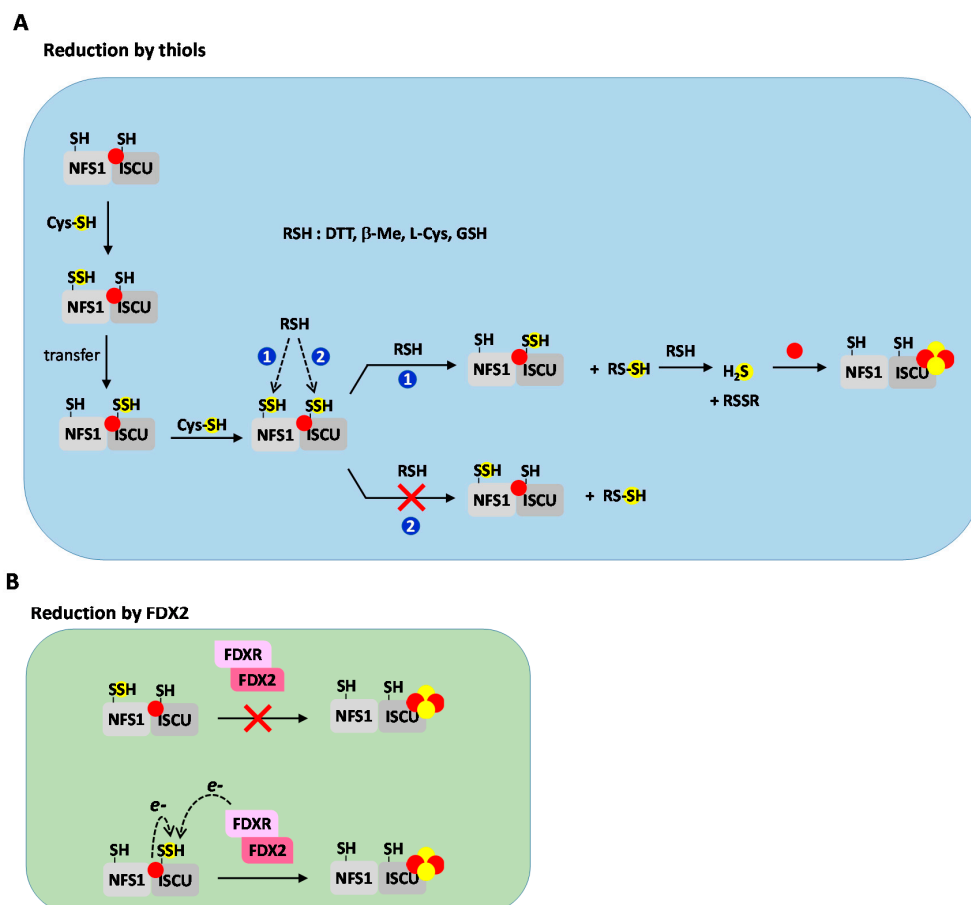


Figure 6. Selective reduction of the persulfide of NFS1 and ISCU by thiols and FDX2. (A) Thiols (RSH) such as dithiothreitol (DTT), L-cysteine, β -mercaptoethanol and GSH react with the persulfide of NFS1. Once a persulfide is formed it is transferred to ISCU, then a second persulfide is formed on NFS1. Thiols reduce the persulfide of NFS1 (**reaction 1**), which generates free persulfidated thiol (RSSH) that reacts with a second molecule of thiol to liberate sulfide ions in solution. Sulfide exists as H_2S , HS^- and S^{2-} depending on the pH, with HS^- the predominant form at physiological pH (pH \approx 8 in mitochondria). The sulfide ions react with iron to generate [2Fe2S] and [4Fe4S] clusters in ISCU. In contrast, the persulfide of ISCU is poorly reactive with thiols (**reaction 2**, the red cross indicates that the reaction does not occur), most likely due to the presence of the metal ion that shields Cys104. Thereby, sulfide ions originate mainly from reduction of NFS1. The dashed black arrows describe the reaction of the thiols on the persulfide of either NFS1 or ISCU (B) FDX2 does not reduce the persulfide of NFS1 (top, the red cross indicates that the reaction does not occur), but selectively reduces the persulfide of ISCU when iron is present in the assembly site (bottom). A mechanism is proposed in which FDX2 provides one electron and the ferrous iron of ISCU the second one to reduce the S-S bond of the persulfide. The dashed black arrows show the origins of these two electrons.

Interestingly, the reduction of the persulfide of ISCU by FDX2 is abolished in the absence of metal and when zinc is present instead of iron in ISCU, which points to a specific role of iron in the reduction process. A mechanistic rationale could be that the iron ion participates as a redox partner. The iron ion is initially ferrous and ends-up as ferric in the $[2\text{Fe}_2\text{S}]^{2+}$ cluster, thereby it might provide one of the two electrons needed to reduce the persulfide, the other one would be delivered by FDX2 (Figure 6B). Altogether, these data support the hypothesis that the reduction of the persulfide of ISCU is specifically coordinated with the presence of iron, which would ensure that the nascent sulfide is instantly trapped by the iron ion. In the SAXS-based model of the *C. thermophilum* ISC complex, the $[2\text{Fe}_2\text{S}]$ cluster of FDX is located nearby the assembly site of ISCU, thus in a suitable position to transfer electrons to the metal center for persulfide reduction [67]. Finally, the titrations of the number of persulfide reduced by FDX2 indicated that only one sulfide is produced per iron-loaded monomer of ISCU [23]. Hence, the most reasonable hypothesis is that the product of the reaction is a mononuclear iron–sulfide ($[1\text{Fe}_1\text{S}]$) species. A number of non-heme mononuclear iron–sulfide inorganic complexes have been reported, thus providing credence to the formation of the same type of species in IscU/ISCU; however, a clear demonstration is still awaited [180–184].

In conclusion, the FDX2-driven reduction of the persulfide on iron-loaded ISCU appears as a concerted process that coordinates sulfide production with presence of iron, which concomitantly prevents escape of the sulfide ions. For these reasons, it has been proposed that the FDX2-based mechanism describes the physiological process of Fe–S cluster assembly [23]. This represents the second encounter of iron and sulfur in the Fe–S cluster assembly process. It is likely that a similar concerted mechanism occurs in the bacterial system, but it has not been demonstrated as of yet. Finally, these data highlight that thiols cannot be considered as surrogates of FDX2 in Fe–S cluster reconstitution assays, as they reduce the persulfide of NFS1, whereas FDX2 reduces the persulfide of ISCU; thus, the mechanisms of sulfide production are completely different. Furthermore, persulfide reduction by thiols is not coupled with the presence of iron.

3.4. Step 4: Fe–S Cluster Formation

The last step, after reduction of the persulfide, is the formation of the $[2\text{Fe}_2\text{S}]$ cluster. This requires formation of a dinuclear iron center with a di- μ -sulfido bridge. Since the titration of persulfides with the mouse system point to the formation of a mononuclear $[1\text{Fe}_1\text{S}]$ iron–sulfide complex, dimerization of IscU/ISCU is likely an obligatory step to form the dinuclear $[2\text{Fe}_2\text{S}]$ cluster (Figure 7). The dimerization would generate a bridged $[2\text{Fe}_2\text{S}]$ cluster, as observed with glutaredoxins that are involved in Fe–S cluster transfer [185–188]. In the reconstitutions performed with *C. thermophilum* Isu1, the final product was a $[2\text{Fe}_2\text{S}]$ cluster in a dimer of Isu1. However, this stoichiometry is also consistent with an asymmetric configuration in which only half of the subunits are occupied [24]. In contrast, a monomer of ISCU carrying one $[2\text{Fe}_2\text{S}]$ cluster has been identified by native mass spectrometry and Mössbauer spectroscopy as the final product in reconstitution assays performed with the mouse ISC system [23]. Therefore, if a bridged $[2\text{Fe}_2\text{S}]$ cluster is formed, it is a transient species that rapidly relocates on one of the subunits (Figure 7) [23]. Then, the dimer dissociates to release the monomer of ISCU holding a $[2\text{Fe}_2\text{S}]$ cluster.

An appealing hypothesis is that the dimeric structure of cysteine desulfurases assists the dimerization of IscU/ISCU within the complex. In the closed conformation of the human NFS1–ISD11–ACP–ISCU complex, the ISCU proteins are very distant (Figure 3A) [67,150], but in its open conformation, the predicted binding sites for ISCU are adjacent and the ISCU proteins are arranged along a C2 axis (Figure 3D) [151], thus in suitable positions for dimerization and formation of a dinuclear center. However, further tightening of the NFS1 subunits would be required to allow contact of the ISCU proteins, so it is not clear whether a dimer could actually form. In contrast, formation of dimers of holo-IscU/ISCU have been reported in several thiol-based reconstitutions [62,81,189,190]. Even a trimeric state has been crystallized with *Aquifex aeolicus* IscU, in which only one subunit harbors a $[2\text{Fe}_2\text{S}]$ cluster [64]. Fe–S reconstituted IscU proteins from *T. maritima* and *A. vinelandii* were shown to

bind one [2Fe2S] cluster per dimer that could correspond to a bridged [2Fe2S] cluster [61,62]. However, the analysis by Mössbauer, electronic absorption and Raman spectroscopies led to the conclusion that the [2Fe2S] cluster in both species is coordinated in an asymmetric environment by the three cysteines Cys35, Cys61, Cys104 and most likely the aspartate Asp37. Since a bridged [2Fe2S] cluster is expected to be symmetric, this asymmetric arrangement indicates that the [2Fe2S] cluster is not bridged but hosted in one of the two subunits of the dimer. A similar signature was observed for the [2Fe2S] cluster in mouse ISCU, which is a key feature indicating that the [2Fe2S] is ligated by a monomer of ISCU [23].

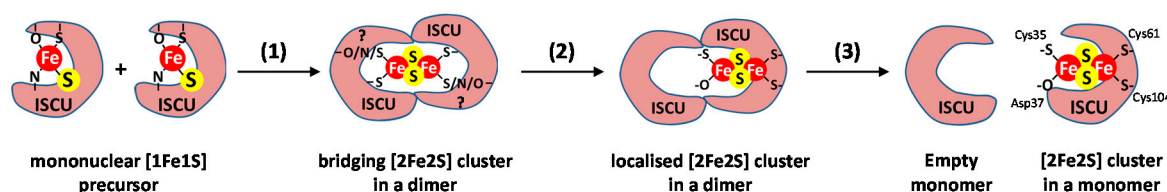


Figure 7. Hypothetic model for the formation of the [2Fe2S] cluster by dimerization of IscU/ISCU. The model for the formation of a [2Fe2S] cluster in IscU/ISCU is decomposed in three steps: (1) the dimerization of two ISCUs coordinating a mononuclear [1Fe1S] intermediate generates a bridged [2Fe2S] cluster in a dimer of ISCU, (2) the [2Fe2S] segregates on one monomer and (3) the dimer dissociates to yield an empty monomer and a monomer containing the [2Fe2S] cluster. In the monomer, the [2Fe2S] cluster is coordinated by Cys35, Asp37, Cys61 and Cys104 of ISCU.

Interestingly, the kinetic analysis of the thiol-based Fe–S cluster assembly process with *A. Vinelandii* IscU showed that the dimer loaded with one [2Fe2S] cluster is a precursor of the dimer loaded with two [2Fe2S] clusters [61]. Therefore, the second [2Fe2S] cluster seems to be assembled by gathering of two iron and two sulfide ions in the empty subunit of the dimer loaded with one [2Fe2S] cluster, thus without requirement for a bridged [2Fe2S] cluster. A similar mechanism was recently proposed for GSH-based Fe–S cluster assembly with *E. coli* IscU [78]. It thus seems that the non-physiological DTT-based route proceeds via sequential accumulation of iron and sulfide ions on a single subunit of dimeric IscU/ISCU while the physiological FDX2-based route involves formation of a still ill-defined transient bridged [2Fe2S] cluster.

In conclusion, although a bridged [2Fe2S] cluster has not been isolated, the ability of IscU/ISCU to dimerize provides credence to a mechanism based on merging of two mononuclear [1Fe1S] precursors. The conformational flexibility of the NFS1–ISD11–ACP complex further raises the possibility that NFS1 could promote dimerization of ISCU, but it is unclear whether bacterial IscS are also capable of such a structural change.

3.5. Regulation of Fe–S Cluster Assembly by Frataxin

3.5.1. Effect of Frataxin on Cysteine Desulfurase Activity: The Key Question of the Rate-Limiting Step

The Pastore group reported that the bacterial frataxin homolog, CyaY, modulates the activity of IscS in the IscS–IscU complex [160]. CyaY decreases the rate of L-alanine production, the by-product of the desulfurization process and this was correlated with a concomitant decrease in the rate of Fe–S cluster production by the IscS–IscU complex in a DTT-based reconstitution. Moreover, the inhibitory effect of CyaY was more pronounced in the presence of iron. Thereby, a function as a gate-keeper preventing uncontrolled production of sulfide ions in the absence of iron, was proposed. In contrast, in DTT-based reconstitutions with the human and mouse ISC system, the eukaryotic frataxin protein (FXN) stimulates the cysteine desulfurase activity of NFS1 [88,164,191]. Moreover, it was shown that the stimulatory effect of FXN is only seen in the presence of ISCU [88,164,191]. These data thus indicate that frataxin affects the activity of cysteine desulfurases in the IscS/NFS1–IscU/ISCU complex, but in different ways depending on the organism.

Several groups have thus studied the cysteine desulfurase activity in more details to determine the kinetic parameters of this reaction [88,158,162–164,191–194]. Most of these assays were conducted in multiple turnover kinetics by monitoring the rates of sulfide or L-alanine productions in the presence of DTT to reduce the persulfide of NFS1 (Figure 8A) [88,158,162–164,191–194]. In multiple turnover kinetics, the rate-limiting step (i.e., the slowest step) dictates the global rate of the reaction. As the cysteine desulfurase assay encompasses two main reactions: persulfide formation (Figure 8A, reaction 1) and persulfide reduction (Figure 8A, reaction 2), either of these reactions could be rate-limiting. In some studies, saturation behaviors were apparently observed upon increase of L-cysteine, which was interpreted as formation of a complex between L-cysteine and NFS1 for persulfide formation (Figure 8A, reaction 1) [158,162–164,191–193]. Since L-cysteine was thought to be involved only at the first step, it was assumed that persulfide formation is the rate-limiting step. Thereby, the effects of FXN and CyaY were interpreted as a modulation of the rate of persulfide formation. The Michaelis–Menten formalism was applied and K_M and k_{cat} values were reported.

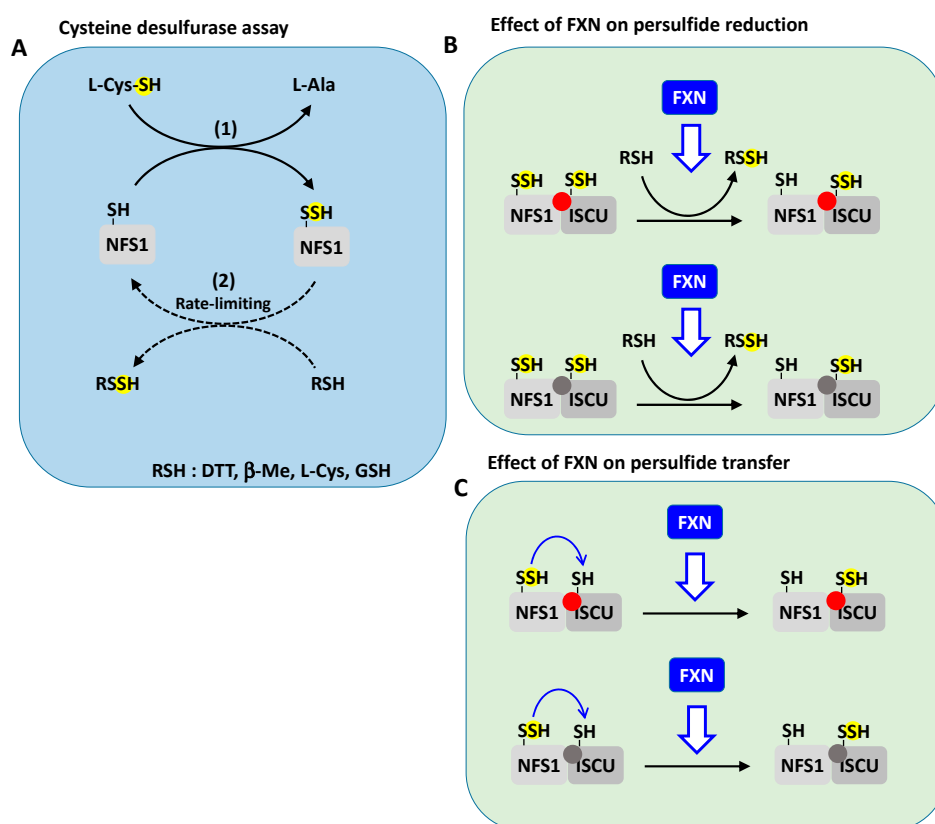


Figure 8. Effect of FXN on persulfide reduction and transfer. (A) The cysteine desulfurase assay encompasses two reactions: (1) formation of the persulfide and (2) its reduction by thiols (RSH). Reduction by thiols is the slowest step (rate-limiting step, dashed black arrows). (B) FXN accelerates the reduction of the persulfide of NFS1 by thiols in the NFS1–ISCU complex with ISCU metallated by iron (red ball) or zinc (gray ball). (C) FXN accelerates the transfer of the persulfide of NFS1 to ISCU in the NFS1–ISCU complex with ISCU metallated by iron (red ball) or zinc (gray ball). The solid blue arrow describes the transfer of persulfide. The blue arrows filled in white refer to acceleration by FXN.

However, a clear demonstration that persulfide formation is rate-limiting in those assays was not provided. Two kinetic studies have addressed the question of the rate-limiting step, with mouse NFS1 and *Synechocystis* IscS [88,195]. In both cases, the rate of L-alanine production was found proportional to the concentration of DTT and additionally to TCEP and β-mercaptoethanol in the case of *Synechocystis* IscS. Since DTT, TCEP and β-mercaptoethanol are not involved in the formation of the persulfide but in its reduction, this indicates that the reduction is the rate-limiting step. Second, it was shown that

L-cysteine is also able to reduce the persulfide of NFS1, thus that the saturation behaviors previously observed could also be interpreted as formation of a complex between L-cysteine and persulfidated NFS1 at the second step (Figure 8A, reaction 2) [88].

A definitive proof that reduction is the rate-limiting step was provided by monitoring persulfide formation and reduction independently in single turnover kinetics with the mouse NFS1–ISD11–ACP complex, using an alkylation assay to quantify protein bound persulfides [88]. Our group showed that persulfide formation is much faster than its reduction by DTT, hence that persulfide reduction, not its formation, is rate-limiting. Moreover, FXN was shown to directly accelerate persulfide reduction by DTT and to the same order of magnitude as its stimulatory effect on the global cysteine desulfurase activity, which further strengthens that persulfide reduction is the rate-limiting step (Figure 8B). Consequently, the ability of FXN to modulate the cysteine desulfurase activity of NFS1 indicates that it facilitates the reduction of the persulfide of NFS1 by thiols (Figure 8A reaction 2, Figure 8B). Even though other studies reported that FXN modulates the rate of persulfide formation, as this reaction is not rate-limiting, this effect of FXN is not expected to impact the cysteine desulfurase activity of NFS1 [89,194].

Moreover, no saturation behavior was observed with mouse NFS1 at low L-cysteine concentrations that could be consistent with the K_M and k_{cat} values reported in other studies [88]. Saturation curves were observed but at high, non-physiological, L-cysteine concentrations (above 50 mM). This was attributed to inhibitory effects by L-cysteine and/or DTT in other systems [43,195]. Anomalous behaviors were also reported for IscS and NifS from *E. coli* and *A. vinelandii*, which precluded determination of the kinetic parameters using the Michaelis–Menten formalism [41,43,196,197]. Altogether, this indicates that persulfide reduction does not proceed through formation of an enzyme-substrate complex but is a bimolecular reaction and that determination of K_M and k_{cat} for L-cysteine is not applicable [88].

Similar extensive studies have not been carried out yet with the *E. coli* system. However, the analysis of *Synechocystis* IscS affords evidence that persulfide reduction is also rate-limiting with a bacterial protein, which suggests that this could be a common feature of class I cysteine desulfurases. This would indicate that CyaY and FXN have opposite effects. However, this differential effect is rather due to the nature of the cysteine desulfurase, since exchanging IscS for the NFS1–ISD11–ACP complex turns CyaY into an activator [163]. Altogether, these data indicate that FXN, and probably CyaY too, modulates the rate of persulfide reduction by DTT and other thiols. However, as discussed in the previous sections, the thiol-based reaction is not physiologically relevant, which means that the effects of FXN and CyaY on the reduction of the persulfide of NFS1 by thiols are unrelated to Fe–S cluster biosynthesis in vivo.

3.5.2. Effect of Frataxin on Persulfide Transfer

Strikingly, assays of persulfide transfer and ^{35}S labeling experiments showed that mouse and human FXN have a strong impact on persulfide transfer to ISCU (Figure 8C) [23,88,158]. Mouse FXN was shown to enhance the rate of this reaction with both Zn–ISCU and Fe–ISCU (Figure 8C) [23,88]. The acceleration with Fe–ISCU was directly correlated to its stimulatory effect on Fe–S cluster assembly in FDX2-based reconstitution assays since persulfide transfer was identified as the rate-limiting step of the whole process [23]. Therefore, the sole function of mammalian FXN that appears relevant to the stimulation of the FDX2-based Fe–S cluster biosynthesis is the stimulation of persulfide transfer.

These data raise the question of the mechanism by which FXN stimulates persulfide transfer. Interestingly, the acceleration of persulfide transfer by FXN is metal-dependent as is persulfide transfer itself, with zinc and iron equally efficient [23]. This strengthens the idea that FXN accelerates the reaction, but does not modify its overall mechanism. The structure of the pentameric NFS1–ISD11–ACP–ISCU–FXN complex with zinc in the assembly site shows that FXN induces a rearrangement of the coordination sphere of the zinc ion (Figure 2C) [73]. The asparagine N141 and the Trp155–Arg165 pair of FXN tears out Cys35 and His103 from the metal ion through specific interactions. The movements induced by FXN thus seems to open the access to Cys104 by pushing aside Cys35 and

His103. Moreover, Cys104 comes closer to the metal ion as His103 is pulled out. Altogether, this may facilitate direct persulfide transfer to Cys104. However, FXN also interacts with the flexible loop of NFS1 and stabilizes the catalytic Cys381 halfway between the PLP and ISCU, which is difficult to rationalize with the stimulation of persulfide transfer and even persulfide formation on NFS1 [73]. However, this position should correspond to an intermediate state since the flexible loop needs to move back to the PLP pocket for persulfide loading.

Another important feature of the stimulation provided by FXN is that it does not modify the nature of the Fe–S cluster formed, i.e., a [2Fe2S] cluster [23]. This behavior fits the notion of a kinetic activator or an co-enzyme rather than an allosteric modulator as earlier proposed [162]. The term “allos” indeed comes from the ancient Greek “ἄλλος”, meaning “other”, and, thus, “allostery” applies to regulators that do not bind to the active site of the enzyme but at another site to modulate its activity, while FXN actually binds to the active site of the ISCU protein.

3.6. Toward a Model of [2Fe2S] Cluster Biosynthesis by the ISC Machinery

Altogether, the current data provide a more complete picture of the mechanism of Fe–S cluster assembly by the ISC machinery. Figures 9–11 depict the models based on these data. Since most mechanistic information originates from the eukaryotic systems, essentially the mouse and human ones, the mammalian nomenclature is used here to describe the mechanisms. Nonetheless, several features of the bacterial machineries suggest that the mechanism of Fe–S cluster assembly is conserved across species. A first striking conclusion is that Fe–S clusters can be assembled via two different routes: the FDX2-based reaction that is physiologically relevant (Figures 9 and 10) and the thiol-based one that is also productive of Fe–S clusters, but only in vitro and is thus not considered as physiologically relevant (Figure 11) [23]. The second breakthrough is the elucidation of the first steps of the FDX2-based reaction leading to production of the sulfide ions and its encounter with iron. The next steps are more elusive. The formation of a dinuclear [2Fe2S] cluster is supposed to rely on dimerization of ISCU and two mechanisms are postulated: either ISCU dimerizes within the complex with assistance from NFS1 (Figure 9) or the NFS1–ISCU complex dissociates and ISCU auto-dimerizes (Figure 10).

The first steps of the FDX2-based reaction are common to both hypothesis (Figures 9 and 10). The reaction is initiated by insertion of a ferrous iron in the assembly site of ISCU, which may require a still ill-defined metallochaperone to remove the zinc ion. It is unclear whether zinc removal and iron insertion in ISCU occur in the NFS1–ISCU complex or in free ISCU, or both. The iron site of ISCU is mononuclear and iron is stable as a high spin Fe(II) center. Upon formation of a complex with the cysteine desulfurase NFS1, a persulfide is transferred to the Cys104 of ISCU, in an iron dependent manner. This iron-assisted reaction allows synchronization of sulfur supply with the presence of iron. This mechanism is referred to the iron-first model since iron comes first then sulfur. Then, FDX2 reduces the persulfide bound to ISCU. The reduction is also iron-dependent, which probably ensures that the production of the sulfide ion is coordinated with the presence of iron, thereby allowing the iron center to trap the nascent sulfide ion.

The reduction by FDX2 would lead to a mononuclear [1Fe1S] species and the dimerization of ISCU would enable formation of a bridged dinuclear [2Fe2S] cluster, either within the NFS1–ISCU complex (Figure 9, internal dimerization) or as a free protein upon dissociation of the NFS1–ISCU complex (Figure 10, external dimerization). In both cases, the transient inter-subunit [2Fe2S] cluster would quickly segregate on one monomer and the chaperone/co-chaperone system HSPA9/HSC20 would enable the transfer of the [2Fe2S] cluster to client proteins. A last important feature of the FDX2-based process is that the rate of Fe–S cluster biosynthesis is controlled by frataxin that accelerates persulfide transfer, the rate-limiting step of the whole process.

Physiological process of Fe-S cluster biosynthesis, NFS1-assisted dimerization of ISCU

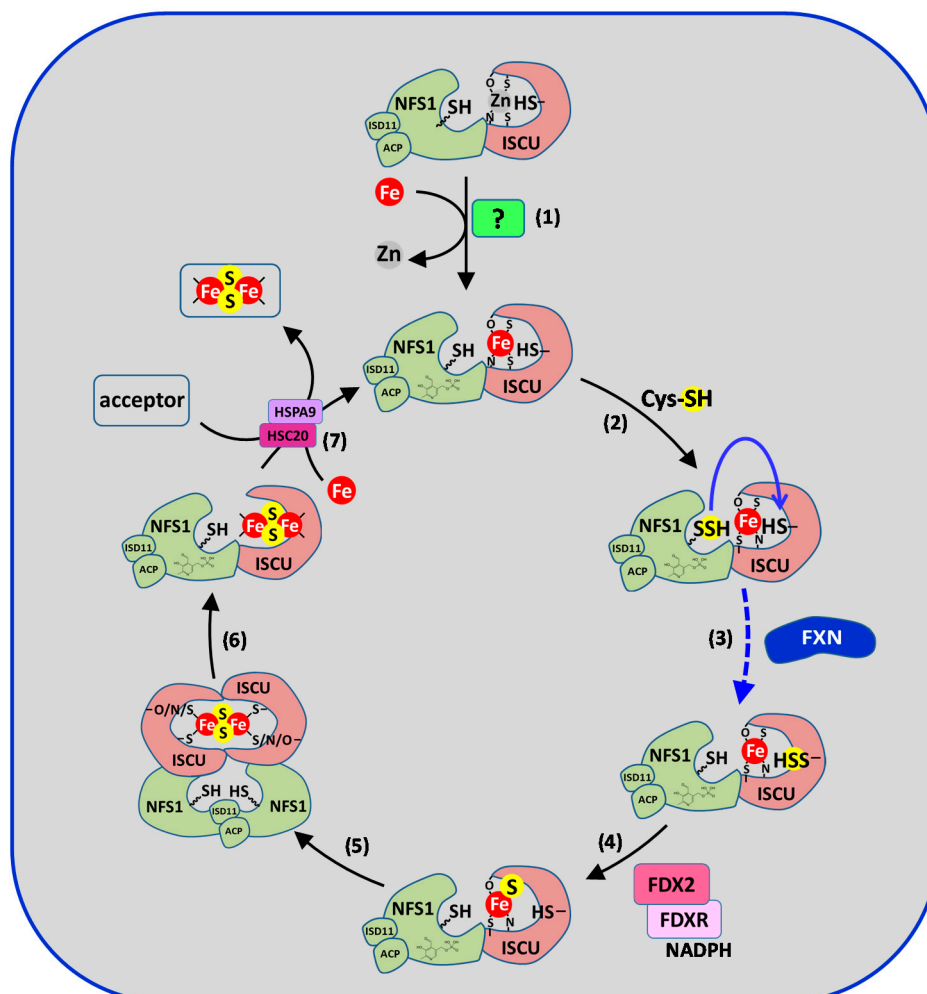


Figure 9. Model of FDX2-based Fe-S cluster biosynthesis by the eukaryotic ISC machinery relying on NFS1-assisted dimerization of ISCU. The reaction is initiated by insertion of iron in apo-ISCU, which may require a still ill-defined metallochaperone to remove the zinc ion (1). In the complex formed with NFS1-ISCU, a persulfide is formed on NFS1 (2) and transferred to ISCU (3). The persulfide of ISCU is reduced by FDX2, possibly into a mononuclear iron-sulfide intermediate (4). Then NFS1 in its open conformation enables the dimerization of ISCU, which leads to formation of a bridged [2Fe2S] cluster in ISCU (5). The bridged [2Fe2S] cluster segregates on one subunit (6) and is transferred to client proteins by the HSC20/HSPA9 chaperone system while a ferrous iron is inserted into apo-ISCU (7). FXN stimulates the whole reaction by accelerating persulfide transfer to ISCU (3). The solid blue arrow describes sulfur transfer to ISCU and the dashed blue arrow refers to the rate-limiting step that is accelerated by FXN.

**Physiological process of Fe-S cluster biosynthesis,
dimerization of free ISCU**

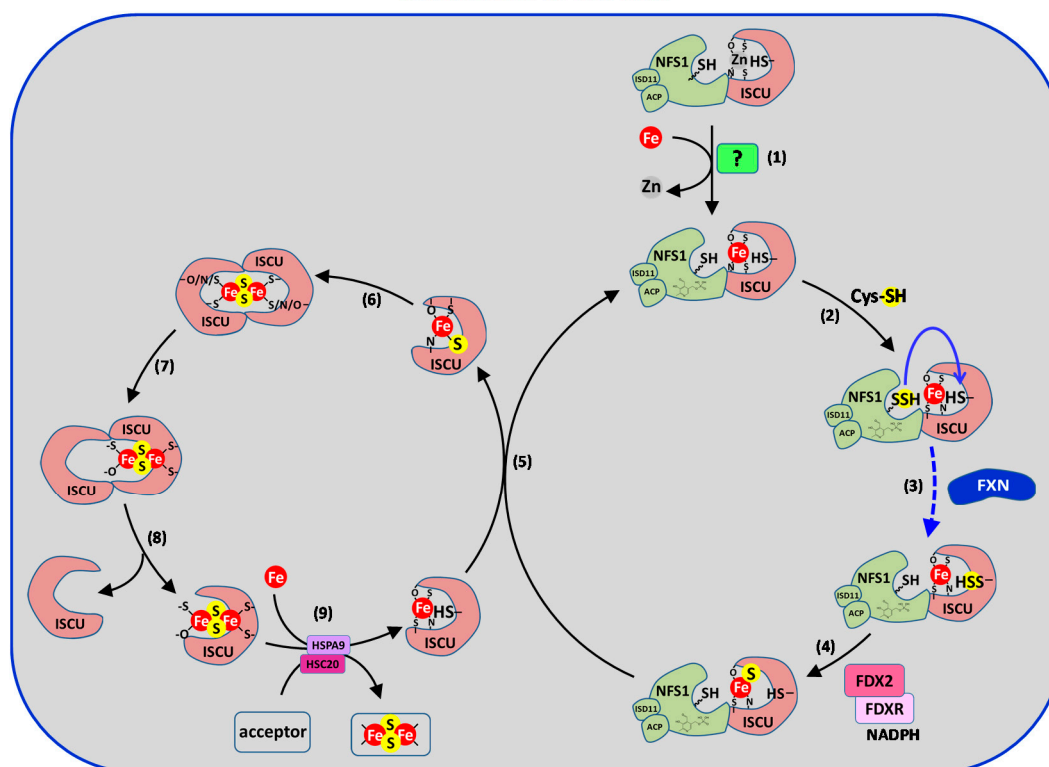


Figure 10. Model of FDX2-based Fe-S cluster biosynthesis by the eukaryotic ISC machinery relying on dimerization of free ISCU. Steps (1)–(4) are common to the mechanism described in Figure 9 until formation of the putative mononuclear iron–sulfide intermediate ([Fe–S]). Then [1Fe1S]-loaded ISCU dissociates from NFS1 either by exchange with Fe-loaded ISCU or spontaneously (5), which allows dimerization of ISCU and formation of a bridged [2Fe2S] cluster (6). The bridged [2Fe2S] cluster segregates on one subunit (7) and the dimer dissociates (8). The monomer of [2Fe2S]-loaded ISCU is recognized by the HSC20/HSPA9 chaperone system which enables the transfer of the [2Fe2S] cluster to client proteins while a ferrous iron is inserted into apo-ISCU (9). FXN stimulates the whole reaction by accelerating persulfide transfer to ISCU (3). The solid blue arrow describes sulfur transfer to ISCU and the dashed blue arrow refers to the rate-limiting step that is accelerated by FXN.

A distinct reaction occurs when thiols are used instead of Fdx/FDX2 as a reducing agent (Figure 11). Thiols such as DTT, GSH and L-cysteine reduce the persulfide of IscS/NFS1, which leads to release of sulfide ions in solution. The sulfide ions then combine with iron, either in solution or in the assembly site, to form [2Fe2S] and [4Fe4S] clusters. This process is not considered as physiologically relevant since production of sulfide is not confined to IscU/ISCU and is not synchronized with the presence of iron. In a biological context, the sulfide ions will diffuse outside of the ISC complex and the likelihood of iron and sulfur encounter will be very low.

However, the thiol-based reduction may compete with sulfur delivery to IscS/ISCU and thus could impede Fe–S cluster assembly. Moreover, in eukaryotes, FXN accelerates this reaction. Since the rate of the thiol-based reduction is proportional to the concentration of the thiol, the turning point at which this reaction starts to compete with Fe–S cluster assembly relies on its concentration. The relevant thiols that should be considered are the most abundant ones in the cells, i.e., GSH (5–10 mM) and L-cysteine (≈ 0.1 mM) [198–200]. Based on the kinetic constants determined for mouse NFS1 with GSH and L-cysteine, the thiol-based reduction would compete with transfer at concentrations of GSH and L-cysteine of 1 M and 15 mM, respectively, thus far from their physiological concentrations [88]. It is thus unlikely that persulfide reduction could compete with persulfide transfer *in vivo*.

Non-physiological process of Fe-S cluster synthesis, thiol-based reaction

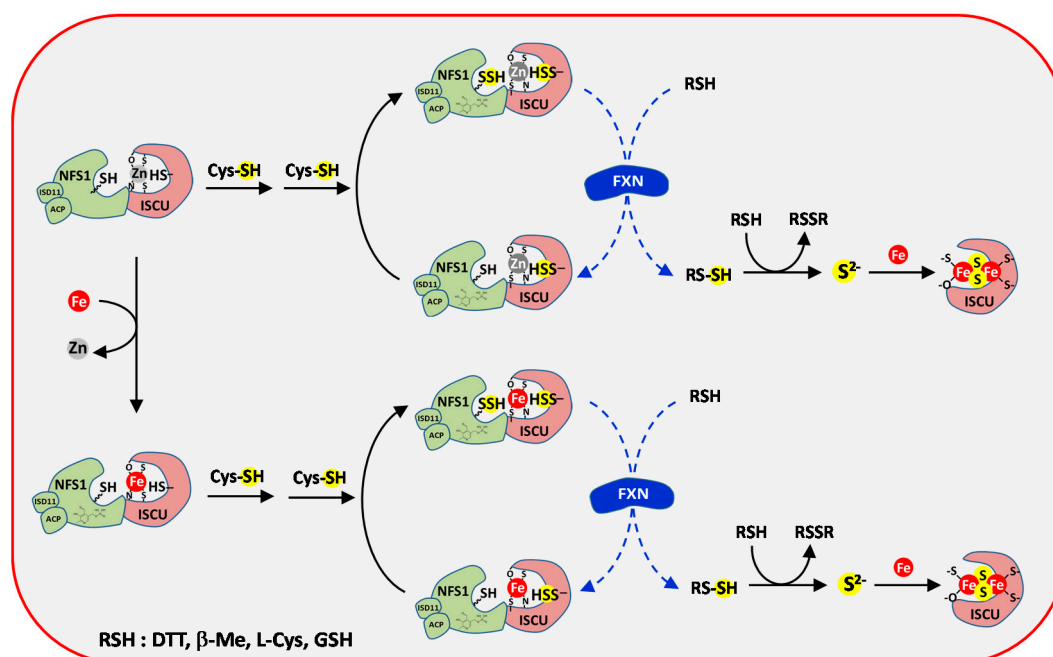


Figure 11. Thiol-based Fe-S cluster synthesis by the eukaryotic ISC machinery. The thiol-based reaction is described for the zinc- and iron-loaded ISC. In both cases, the reaction is initiated by formation of an NFS1-ISP11-ACP-ISC complex persulfidated on both NFS1 and ISC, then thiols, (RSH) such as L-cysteine, DTT, GSH or β -mercaptoethanol, reduce the persulfide of NFS1, which leads to sulfide release. In the presence of iron, the sulfide ions generate Fe-S clusters in ISC via a poorly defined mechanism. The dashed blue arrows refer to the rate-limiting steps that are accelerated by FXN.

4. Fe-S Assembly by the NIF Machinery

4.1. Iron Insertion in NifU

The NIF machinery comprises two main proteins, the scaffold protein NifU and the cysteine desulfurase NifS. NifU is a modular protein containing three distinct domains [36,41,201]. An N-terminal domain with very high homology to IscU/ISCU, a central domain harboring a permanent [2Fe2S] cluster homolog to ferredoxin and a C-terminal domain called NfU that has been proposed to function as a scaffold of [4Fe4S] clusters and a Fe-S cluster carrier.

The N-terminal domain contains all the well-conserved amino acids that bind the ferrous iron in IscU/ISCU: Cys35, Asp37, Cys61 and His103. It also contains the persulfide receptor Cys104 [23]. The N-terminal domain of NifU was shown to bind a mononuclear iron ion, most likely via Cys35, Cys61 and Cys104. However, in contrast to IscU/ISCU iron binds in the ferric state and Asp37 is not involved in its coordination [201]. Moreover, binding of Fe^{3+} to NifU is only observed below 2 °C, which questions its role in Fe-S cluster biosynthesis. In another study, time-course analysis by Mössbauer spectroscopy suggested that ferrous iron binds to NifU in a cysteine-rich site, which may correspond to the assembly site of the N-terminal IscU/ISCU domain [38]. Thereby an iron-first mechanism may also apply to NifU as reported for IscU/ISCU.

4.2. Still Elusive Steps Leading to Formation of the [2Fe2S] and [4Fe4S] Clusters

It is still unclear how NifU acquires sulfur. Although NifU and NifS form a complex, persulfide transfer to NifU has not been reported. Yet NifS-mediated Fe-S cluster reconstitutions in NifU were reported in DTT-based assays, which provide an idea of which domain binds Fe-S clusters. A truncated form of NifU containing only its N-terminal domain was shown to assemble a labile

[2Fe2S] cluster, as observed for IscU/ISCU [202]. Time-course experiments further suggested that this [2Fe2S] is converted into a [4Fe4S] cluster by reductive coupling [38]. However, as these reactions were performed with DTT as a reductant, it is still unclear whether assembly of [4Fe4S] clusters by the N-terminal domain is physiologically relevant. Moreover, no reductase has been identified in the NIF operon that could achieve the reduction of a persulfide transferred to NifU. An appealing hypothesis is that the permanent [2Fe2S] cluster of the central domain of NifU fills up this function, as described for FDX2. NifU may thus combine the functions of IscU/ISCU and Fdx/FDX2 within the same polypeptide for the biosynthesis of [2Fe2S] clusters.

Fe–S cluster reconstitution assays with the full-length NifU protein afforded evidence that the NfU domain binds [4Fe4S] clusters [38]. The formation of [4Fe4S] clusters is supposed to proceed via reductive coupling of two [2Fe2S] clusters and ferredoxin is able to catalyze this type of reaction [203]. As no reductase has been identified in the NIF operon, the permanent [2Fe2S] cluster of NifU may also fulfill this function. Thereby, the permanent [2Fe2S] cluster might play a bifunctional role, in persulfide reduction and in reductive coupling of the [2Fe2S] clusters. This process would require an external reductase to deliver electrons to the permanent [2Fe2S] cluster, but as for the ISC machinery, this reductase may not be encoded by the NIF operon. In analogy with NfU homologs that are involved in the assembly and/or transfer of [4Fe4S] clusters, the NfU domain of NifU might be the place for reductive coupling of the [2Fe2S] clusters leading to formation of the [4Fe4S] cluster [6].

5. Fe–S Assembly by the SUF Machinery

5.1. Overall Description of the SUF Machinery

There are several striking differences between the ISC and SUF machineries that are likely related to the higher resistance of the SUF machinery under stress conditions [26]. As the description of the SUF machinery has been extensively reviewed in other reports, the reader is referred to these reviews for more details [26,47,204]. We attempt, here, to focus on comparative elements between the ISC and SUF machineries.

Like the ISC machinery, the genes encoding the components of the SUF machinery are organized in operons [47]. The SUF system contains two to six genes depending on the organisms. The main components are SufS, the cysteine desulfurase providing sulfur and a scaffolding complex formed by the SufB, SufD and SufC proteins. Complexes containing various stoichiometries of the SufB, SufD and SufC proteins can be isolated by mixing the purified proteins *in vitro*, but the physiologically active complex is most likely a SufBC₂D complex [26,205]. The crystal structure of the SufBC₂D complex shows that SufB and SufD form a heterodimer with two SufC proteins bound to each subunit [206]. The site of Fe–S cluster assembly has been localized at the interface of the SufB–SufD heterodimer with Cys405, Glu434 or Glu432 and His433 from SufB and His360 from SufD as putative ligands of the Fe–S cluster [26]. SufC is an ATPase that drives structural changes to the SufB–SufD complex for proper Fe–S cluster assembly. The SUF operons also encode SufE or SufU, two sulfur relay proteins shuttling the persulfide generated by SufS to the scaffolding complex. SufE and SufU occur in a mutually exclusive manner in bacterial genomes and can complement each other, which indicates that they play very similar roles [47,207–210].

The persulfide transfer processes involving SufE or SufU have been particularly well studied. In contrast, it is still unclear how and where iron is inserted in the SufBC₂D scaffold and whether or not persulfide supply is coupled with the presence of iron as observed with the ISC machinery. The mechanism of persulfide reduction is also still elusive.

5.2. Iron Insertion in the SufBC₂D Scaffold

The few data available on the process of iron insertion in the SufBC₂D complex suggest distinct mechanisms for the ISC and SUF machineries. Strains lacking SufC are impaired in the utilization of iron and a specific disruption of the ATPase activity of SufC lowers the iron content of the SufBC₂D

complex in vivo [211,212]. These data raise the possibility that SufC is important for iron acquisition by the SufBC₂D complex. An active process relying on the ATPase activity of SufC may provide a rationale to the higher ability of the SUF machinery to cope with iron-poor conditions, as compared to the ISC machinery for which a passive mode of iron insertion is postulated (see Section 3.1.2). Moreover, the SufBC₂D complex was proposed to function as a reductase of ferric iron [205,211]. The SufBC₂D complex isolated from *E. coli* co-purifies with one molecule of reduced FADH₂ per complex. This FADH₂ was shown to mobilize iron from ferric citrate and the ferric-loaded form of CyaY. This suggests that the SUF system is able to mobilize the poorly soluble ferric iron, which could provide a significant advantage under iron-poor conditions. However, the iron-binding site in the SufBC₂D complex has not been yet identified to test these hypotheses.

5.3. Sulfur Insertion in the SufBC₂D Complex

5.3.1. SufS, the Source of Sulfur

SufS belongs to the class II of the desulfurase family that are characterized by a shorter flexible loop carrying the catalytic cysteine [26]. The formation of the persulfide is also slower in class II than in class I, but accelerated by binding of SufU or SufE [26,213]. The reduction of the persulfide of SufS by thiols is apparently rate-limiting as for class I, which emphasizes that the persulfide is largely excluded from solvent [208,213–215]. Thereby, sulfur delivery is confined to the surrounding of the PLP-binding pocket and specific sulfur acceptors (SufE, SufU) are needed to mediate sulfur transfer to the SufBC₂D complex, most likely to ensure shielding of the persulfide.

5.3.2. Sulfur Transfer via SufE

SufE was shown to accept sulfur from SufS on its highly conserved cysteine residue, Cys51 [214,216]. The trans-persulfuration reaction relies on mutual changes in the structure of SufE and SufS [217–224]. The crystal structures of SufE show that the Cys51 is initially buried and protected from the solvent in a hydrophobic pocket [225,226]. Although there is still no tri-dimensional structure of the SufS–SufE complex, deuterium exchange experiments and comparison with the structure of the closely related homolog CsdA–CsdE complex have provided information on the mechanism of persulfide transfer [217–224]. Upon binding of CsdE to CsdA, the loop of CsdE carrying the receptor cysteine is twisted and comes in close proximity of the catalytic cysteine of CsdA, a similar remodeling is hypothesized for the SufS–SufE complex that would facilitate the nucleophilic attack by Cys51 of SufE. In addition, local changes in the SufS catalytic site and dimer interface may promote the desulfurase reaction and an outward-facing position of the persulfidated Cys364. This could provide a way to couple persulfide formation with its transfer. Upon dissociation of the SufS–SufE complex, the persulfide transferred to SufE is protected from the solvent most likely through a backward movement of the flexible to the hydrophobic cavity [225–227].

5.3.3. Sulfur Transfer via SufU

Due to its high homology with IscU/ISCU, SufU was initially proposed to function as a scaffold for Fe–S cluster assembly [209,228]. However, SufU cannot complement the lack of IscU/ISCU, which indicates that these proteins have different roles [159,207,210]. The main structural differences between SufU and IscU/ISCU are an insertion of 18–21 residues between the second and third cysteine residues and the lack of the well-conserved histidine H103 [23]. Since SufU accepts a persulfide from SufS, the current view is that SufU is a sulfurtransferase, as SufE, that conveys the persulfide from SufS to the SufBC₂D complex [208,228,229].

Interestingly, SufU hosts a tightly bound zinc ion that is essential for persulfide transfer [159,230,231]. The structure of SufU proteins revealed that the zinc ion is coordinated in a tetrahedral geometry by the three cysteines Cys41, Cys66, and Cys128 and the aspartate Asp43 (Figure 12A) [230,231]. These residues are equivalent to Cys35, Cys61, Cys104 and the aspartate Asp37 in IscU/ISCU. Upon formation of a

complex with SufS, SufU and SufS undergo major structural changes (Figure 12B) [232,233]. The mobile loop of SufS carrying the catalytic cysteine Cys361 moves freely and the histidine residue His342 of SufS becomes a ligand of the zinc ion of SufU by swapping with the cysteine C41. Consequently, Cys41 is released and directed toward Cys361 of SufS. Soaking of the crystals of the SufS–SufU complex with L-cysteine leads to extra electronic densities at Cys361 and Cys41 consistent with cysteine persulfides, thus suggesting that persulfide transfer occurs between these residues [232].

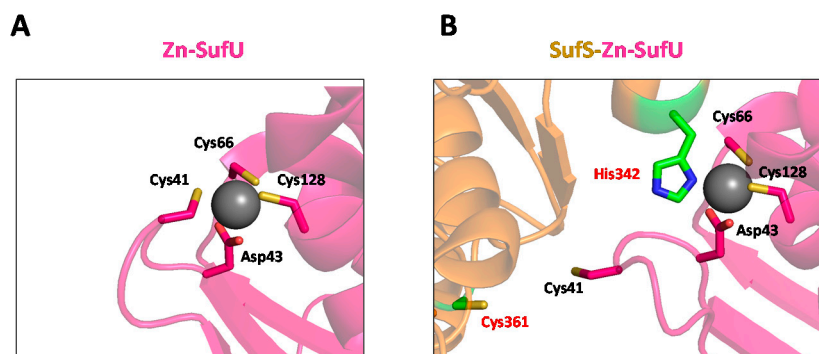


Figure 12. Structural rearrangement at the zinc site of SufU upon binding of SufS. Zoom on the zinc site of (A) *Bacillus subtilis* SufU (PDB 6JZV) and (B) *Bacillus subtilis* SufS–SufU complex (PDB 5XT5). SufU is colored in pink with key amino acids coordinating the zinc ion (Cys41, Asp43, Cys66 and Cys128) and SufS in orange with its catalytic cysteine Cys361 in green. The zinc ion is initially coordinated by Cys41, Asp43, Cys66 and Cys128 of SufU. Upon binding to SufS, His342 of SufS exchanges with Cys41, which comes close by Cys361, the catalytic cysteine of SufS.

This metal-dependent process is reminiscent of the persulfide transfer reaction reported for the NFS1–ISCU complex (Figure 2), but is mechanistically different. The main difference relates to the shorter length of the flexible loop carrying the catalytic cysteine in SufS that does not allow persulfide transfer to the distal cysteine (Cys128) but to a proximal one (Cys41) that is released upon binding of His342 to the zinc ion. This highlights two different ways of using a metal ion for persulfide transfer. In IscU/ISCU, the metal center anchors the persulfide of the desulfurase in close proximity of the receptor cysteine while in SufU, ligand exchange at the metal center expels the receptor cysteine and drives it close to the catalytic cysteine.

5.4. Persulfide Transfer to SufBC₂D and Reduction via FADH₂?

SufE interacts with the SufBC₂D complex and the cysteine Cys254 has been proposed as the primary acceptor in SufB [26,51,227,234]. Then this persulfide would be conveyed to the cysteine Cys405 of SufB through a hydrophobic tunnel involving non-cysteine amino acids as sulfur relays [26,206,234]. In contrast to the ISC machinery, there is, as of yet, no indication that iron is involved or required for persulfide transfer between SufE and SufB and within SufB. Moreover, the assembly site in the SufBC₂D complex is 20 Å away from the entry point of sulfur on Cys254, it is thus still unclear how sulfur insertion could be coupled with presence of iron in the SufBC₂D complex. The sulfur transfer process from SufU to SufBC₂D has not been investigated yet, whether SufU transfers its persulfide to Cys254 as SufE is not known.

The SUF operon does not encode any obvious reductase that could play a role in persulfide reduction. Moreover, *E. coli* strains lacking Fdx that are thus defective in ISC-driven Fe–S cluster assembly, are viable. This indicates that the SUF machinery is active under these conditions and thus that Fdx is not the reductase of this machinery. Therefore, another reductase dedicated to the SUF operon should exist [168,170]. As mentioned above, the SufBC₂D complex isolated from *E. coli* co-purifies with one molecule of reduced FADH₂ per complex [205,211]. Although this cofactor is

proposed to operate as a ferric reductase, it may also provide reducing equivalents for the reduction of the persulfide transferred to the SufBC₂D complex.

6. Concluding Remarks

The recent advances in the field of Fe–S cluster biogenesis have shed new light on the process of their assembly. We are now close to provide a complete picture for the assembly of [2Fe2S] clusters by the ISC machinery. Two key primary steps have been uncovered with the mouse system: persulfide transfer to ISCU and its reduction by FDX2 that are both metal-dependent. This process is most likely conserved in bacteria, but this is still awaiting confirmation. In the first step, iron comes first and enables persulfide insertion in IscU/ISCU. In the second step, persulfide reduction is coupled to the presence of iron. Altogether, these metal dependent steps probably allow allocation of the proper amount of sulfur to the iron center of IscU/ISCU and coordinate sulfide release with the presence of iron to generate the first iron-sulfide link. However, a number of key questions remain to be solved, essentially the mechanism by which persulfide transfer and its reduction are coupled with iron and how the mononuclear center of IscU/ISCU is converted into a dinuclear center to form the [2Fe2S] cluster. By unravelling the primary steps of Fe–S cluster assembly, the functional role of frataxin is also becoming more clear. There is now compelling evidence pointing to a role of frataxin as a kinetic modulator of persulfide transfer.

Since the ISC and NIF systems are very similar in several ways, the data accumulated on the ISC system will likely help unravel the mechanism by which the NIF machinery assembles Fe–S clusters. In contrast, the comparisons of the ISC and SUF systems point to major differences. The persulfide transfer process in the SUF systems is split into discrete steps involving sulfur relay proteins and a trans-persulfuration reaction with the SufBC₂D complex. In the first step, a buried area is created at the interface of the SufS–SufE/U complex, to achieve the trans-persulfuration reaction. This protected area probably shields the persulfide and the reactive cysteines from oxidants. The iron-insertion process also seems very different, but its description is still too elusive to allow a clear description. Several other questions are pending, essentially whether persulfide transfer is coupled with iron insertion, how the persulfide is reduced into sulfide and how the [2Fe2S] cluster is formed. Addressing these questions will improve our understanding of the mechanism by which the SUF machinery copes with iron-poor and oxidative-stress conditions.

Author Contributions: B.D., supervision and review-writing; B.S. writing contributions; S.G., writing contributions, bibliographic resources; B.M., text corrections. All authors have read and agreed to the published version of the manuscript.

Funding: This research was funded by ANR grant (Frataxur, ANR-17-CE11-0021-01) and FARA grant (202212) awarded to B.D., B.M. was funded by FARA grant (202212).

Conflicts of Interest: The authors declare no conflict of interest.

References

1. Camprubi, E.; Jordan, S.F.; Vasiliadou, R.; Lane, N. Iron catalysis at the origin of life. *IUBMB Life* **2017**, *69*, 373–381. [[CrossRef](#)]
2. Huber, C.; Wachtershauser, G. Alpha-Hydroxy and alpha-amino acids under possible Hadean, volcanic origin-of-life conditions. *Science* **2006**, *314*, 630–632. [[CrossRef](#)]
3. Cody, G. Transition metal sulfides and the origin of metabolism. *Annu. Rev. Earth Planet. Sci.* **2004**, *32*, 569–599. [[CrossRef](#)]
4. Martin, W.; Russell, M.J. On the origins of cells: A hypothesis for the evolutionary transitions from abiotic geochemistry to chemoautotrophic prokaryotes, and from prokaryotes to nucleated cells. *Philos. Trans. R. Soc. Lond. B Biol. Sci.* **2003**, *358*, 59–83, discussion 55–83. [[CrossRef](#)]
5. Chahal, H.K.; Boyd, J.M.; Outten, F.W. Iron–Sulfur Cluster Biogenesis in Archaea and Bacteria. In *Encyclopedia of Inorganic and Bioinorganic Chemistry*; Scott, R.A., Ed.; Wiley: Hoboken, NJ, USA, 2013. [[CrossRef](#)]

6. Lill, R.; Freibert, S.A. Mechanisms of Mitochondrial Iron-Sulfur Protein Biogenesis. *Annu. Rev. Biochem.* **2020**, *89*, 471–499. [[CrossRef](#)]
7. Paul, V.D.; Lill, R. Biogenesis of cytosolic and nuclear iron-sulfur proteins and their role in genome stability. *Biochim. Biophys. Acta* **2015**, *1853*, 1528–1539. [[CrossRef](#)]
8. Przybyla-Tosciano, J.; Roland, M.; Gaymard, F.; Couturier, J.; Rouhier, N. Roles and maturation of iron-sulfur proteins in plastids. *J. Biol. Inorg. Chem.* **2018**, *23*, 545–566. [[CrossRef](#)]
9. Roche, B.; Aussel, L.; Ezraty, B.; Mandin, P.; Py, B.; Barras, F. Iron/sulfur proteins biogenesis in prokaryotes: Formation, regulation and diversity. *Biochim. Biophys. Acta* **2013**, *1827*, 455–469. [[CrossRef](#)]
10. Martin, D.; Charpilienne, A.; Parent, A.; Boussac, A.; D'Autreaux, B.; Poupon, J.; Poncet, D. The rotavirus nonstructural protein NSP5 coordinates a [2Fe–2S] iron-sulfur cluster that modulates interaction to RNA. *FASEB J.* **2013**, *27*, 1074–1083. [[CrossRef](#)]
11. Tam, W.; Pell, L.G.; Bona, D.; Tsai, A.; Dai, X.X.; Edwards, A.M.; Hendrix, R.W.; Maxwell, K.L.; Davidson, A.R. Tail tip proteins related to bacteriophage lambda gpL coordinate an iron-sulfur cluster. *J. Mol. Biol.* **2013**, *425*, 2450–2462. [[CrossRef](#)]
12. Tsang, S.H.; Wang, R.; Nakamaru-Ogiso, E.; Knight, S.A.; Buck, C.B.; You, J. The Oncogenic Small Tumor Antigen of Merkel Cell Polyomavirus Is an Iron-Sulfur Cluster Protein That Enhances Viral DNA Replication. *J. Virol.* **2016**, *90*, 1544–1556. [[CrossRef](#)] [[PubMed](#)]
13. Estellon, J.; Ollagnier de Choudens, S.; Smadja, M.; Fontecave, M.; Vandenbrouck, Y. An integrative computational model for large-scale identification of metalloproteins in microbial genomes: A focus on iron-sulfur cluster proteins. *Metallomics* **2014**, *6*, 1913–1930. [[CrossRef](#)]
14. Liu, J.; Chakraborty, S.; Hosseinzadeh, P.; Yu, Y.; Tian, S.; Petrik, I.; Bhagi, A.; Lu, Y. Metalloproteins containing cytochrome, iron-sulfur, or copper redox centers. *Chem. Rev.* **2014**, *114*, 4366–4469. [[CrossRef](#)] [[PubMed](#)]
15. Stegmaier, K.; Blinn, C.M.; Bechtel, D.F.; Greth, C.; Auerbach, H.; Muller, C.S.; Jakob, V.; Reijerse, E.J.; Netz, D.J.A.; Schunemann, V.; et al. Apd1 and Aim32 Are Prototypes of Bishistidinyl-Coordinated Non-Rieske [2Fe–2S] Proteins. *J. Am. Chem. Soc.* **2019**, *141*, 5753–5765. [[CrossRef](#)]
16. Berkovitch, F.; Nicolet, Y.; Wan, J.T.; Jarrett, J.T.; Drennan, C.L. Crystal Structure of Biotin Synthase, an S-Adenosylmethionine-Dependent Radical Enzyme. *Science* **2004**, *303*, 76. [[CrossRef](#)]
17. Bak, D.W.; Elliott, S.J. Alternative FeS cluster ligands: Tuning redox potentials and chemistry. *Curr. Opin. Chem. Biol.* **2014**, *19*, 50–58. [[CrossRef](#)]
18. Hu, Y.; Ribbe, M.W. Biosynthesis of the Metalloclusters of Nitrogenases. *Annu. Rev. Biochem.* **2016**, *85*, 455–483. [[CrossRef](#)] [[PubMed](#)]
19. Dobbek, H.; Svetlitchnyi, V.; Gremer, L.; Huber, R.; Meyer, O. Crystal Structure of a Carbon Monoxide Dehydrogenase Reveals a [Ni–4Fe–5S] Cluster. *Science* **2001**, *293*, 1281. [[CrossRef](#)] [[PubMed](#)]
20. Cooper, S.J.; Garner, C.D.; Hagen, W.R.; Lindley, P.F.; Bailey, S. Hybrid-cluster protein (HCP) from *Desulfovibrio vulgaris* (Hildenborough) at 1.6 Å resolution. *Biochemistry* **2000**, *39*, 15044–15054. [[CrossRef](#)] [[PubMed](#)]
21. Beinert, H. Iron-sulfur proteins: Ancient structures, still full of surprises. *J. Biol. Inorg. Chem.* **2000**, *5*, 2–15. [[CrossRef](#)]
22. Blanc, B.; Gerez, C.; Ollagnier de Choudens, S. Assembly of Fe/S proteins in bacterial systems: Biochemistry of the bacterial ISC system. *Biochim. Biophys. Acta* **2015**, *1853*, 1436–1447. [[CrossRef](#)] [[PubMed](#)]
23. Gervason, S.; Larkem, D.; Mansour, A.B.; Botzanowski, T.; Muller, C.S.; Pecqueur, L.; Le Pavec, G.; Delaunay-Moisan, A.; Brun, O.; Agramunt, J.; et al. Physiologically relevant reconstitution of iron-sulfur cluster biosynthesis uncovers persulfide-processing functions of ferredoxin-2 and frataxin. *Nat. Commun.* **2019**, *10*, 3566. [[CrossRef](#)] [[PubMed](#)]
24. Weibert, H.; Freibert, S.A.; Gallo, A.; Heidenreich, T.; Linne, U.; Amlacher, S.; Hurt, E.; Muhlenhoff, U.; Banci, L.; Lill, R. Functional reconstitution of mitochondrial Fe/S cluster synthesis on Isu1 reveals the involvement of ferredoxin. *Nat. Commun.* **2014**, *5*, 5013. [[CrossRef](#)] [[PubMed](#)]
25. Ciofi-Baffoni, S.; Nasta, V.; Banci, L. Protein networks in the maturation of human iron-sulfur proteins. *Metallomics* **2018**, *10*, 49–72. [[CrossRef](#)]
26. Pérard, J.; Ollagnier de Choudens, S. Iron-sulfur clusters biogenesis by the SUF machinery: Close to the molecular mechanism understanding. *JBIC J. Biol. Inorg. Chem.* **2018**, *23*, 581–596. [[CrossRef](#)] [[PubMed](#)]
27. Rouault, T.A.; Maio, N. Biogenesis and functions of mammalian iron-sulfur proteins in the regulation of iron homeostasis and pivotal metabolic pathways. *J. Biol. Chem.* **2017**, *292*, 12744–12753. [[CrossRef](#)]

28. Delewski, W.; Paterkiewicz, B.; Manicki, M.; Schilke, B.; Tomiczek, B.; Ciesielski, S.J.; Nierzwicki, L.; Czub, J.; Dutkiewicz, R.; Craig, E.A.; et al. Iron-Sulfur Cluster Biogenesis Chaperones: Evidence for Emergence of Mutational Robustness of a Highly Specific Protein-Protein Interaction. *Mol. Biol. Evol.* **2016**, *33*, 643–656. [[CrossRef](#)]
29. Beilschmidt, L.K.; Ollagnier de Choudens, S.; Fournier, M.; Sanakis, I.; Hograindleur, M.A.; Clemancey, M.; Blondin, G.; Schmucker, S.; Eisenmann, A.; Weiss, A.; et al. ISCA1 is essential for mitochondrial Fe₄S₄ biogenesis in vivo. *Nat. Commun.* **2017**, *8*, 15124. [[CrossRef](#)]
30. Brancaccio, D.; Gallo, A.; Mikolajczyk, M.; Zovo, K.; Palumaa, P.; Novellino, E.; Piccioli, M.; Ciofi-Baffoni, S.; Banci, L. Formation of [4Fe–4S] clusters in the mitochondrial iron-sulfur cluster assembly machinery. *J. Am. Chem. Soc.* **2014**, *136*, 16240–16250. [[CrossRef](#)]
31. Brancaccio, D.; Gallo, A.; Piccioli, M.; Novellino, E.; Ciofi-Baffoni, S.; Banci, L. [4Fe–4S] Cluster Assembly in Mitochondria and Its Impairment by Copper. *J. Am. Chem. Soc.* **2017**, *139*, 719–730. [[CrossRef](#)]
32. Muhlenhoff, U.; Richter, N.; Pines, O.; Pierik, A.J.; Lill, R. Specialized function of yeast Isa1 and Isa2 proteins in the maturation of mitochondrial [4Fe–4S] proteins. *J. Biol. Chem.* **2011**, *286*, 41205–41216. [[CrossRef](#)] [[PubMed](#)]
33. Weiler, B.D.; Bruck, M.C.; Kothe, I.; Bill, E.; Lill, R.; Muhlenhoff, U. Mitochondrial [4Fe–4S] protein assembly involves reductive [2Fe–2S] cluster fusion on ISCA1-ISCA2 by electron flow from ferredoxin FDX2. *Proc. Natl. Acad. Sci. USA* **2020**, *117*, 20555–20565. [[CrossRef](#)] [[PubMed](#)]
34. Jacobson, M.R.; Cash, V.L.; Weiss, M.C.; Laird, N.F.; Newton, W.E.; Dean, D.R. Biochemical and genetic analysis of the nifUSVWZM cluster from *Azotobacter vinelandii*. *Mol. Gen. Genet.* **1989**, *219*, 49–57. [[CrossRef](#)]
35. Zheng, L.; White, R.H.; Cash, V.L.; Jack, R.F.; Dean, D.R. Cysteine desulfurase activity indicates a role for NIFS in metallocluster biosynthesis. *Proc. Natl. Acad. Sci. USA* **1993**, *90*, 2754–2758. [[CrossRef](#)] [[PubMed](#)]
36. Fu, W.; Jack, R.F.; Morgan, T.V.; Dean, D.R.; Johnson, M.K. nifU gene product from *Azotobacter vinelandii* is a homodimer that contains two identical [2Fe–2S] clusters. *Biochemistry* **1994**, *33*, 13455–13463. [[CrossRef](#)]
37. Johnson, D.C.; Dos Santos, P.C.; Dean, D.R. NifU and NifS are required for the maturation of nitrogenase and cannot replace the function of isc-gene products in *Azotobacter vinelandii*. *Biochem. Soc. Trans.* **2005**, *33*, 90–93. [[CrossRef](#)]
38. Smith, A.D.; Jameson, G.N.; Dos Santos, P.C.; Agar, J.N.; Naik, S.; Krebs, C.; Frazzon, J.; Dean, D.R.; Huynh, B.H.; Johnson, M.K. NifS-mediated assembly of [4Fe–4S] clusters in the N- and C-terminal domains of the NifU scaffold protein. *Biochemistry* **2005**, *44*, 12955–12969. [[CrossRef](#)]
39. Black, K.A.; Dos Santos, P.C. Shared-intermediates in the biosynthesis of thio-cofactors: Mechanism and functions of cysteine desulfurases and sulfur acceptors. *Biochim. Biophys. Acta* **2015**, *1853*, 1470–1480. [[CrossRef](#)]
40. Leimkühler, S.; Böhning, M.; Beilschmidt, L. Shared Sulfur Mobilization Routes for tRNA Thiolation and Molybdenum Cofactor Biosynthesis in Prokaryotes and Eukaryotes. *Biomolecules* **2017**, *7*, 5.
41. Zheng, L.; Cash, V.L.; Flint, D.H.; Dean, D.R. Assembly of iron-sulfur clusters. Identification of an iscSUA-hscBA-fdx gene cluster from *Azotobacter vinelandii*. *J. Biol. Chem.* **1998**, *273*, 13264–13272. [[CrossRef](#)]
42. Patzer, S.I.; Hantke, K. SufS is a NifS-like protein, and SufD is necessary for stability of the [2Fe–2S] FhuF protein in *Escherichia coli*. *J. Bacteriol.* **1999**, *181*, 3307–3309. [[CrossRef](#)] [[PubMed](#)]
43. Mihara, H.; Kurihara, T.; Yoshimura, T.; Esaki, N. Kinetic and mutational studies of three NifS homologs from *Escherichia coli*: Mechanistic difference between L-cysteine desulfurase and L-selenocysteine lyase reactions. *J. Biochem.* **2000**, *127*, 559–567. [[CrossRef](#)] [[PubMed](#)]
44. Nachin, L.; El Hassouni, M.; Loiseau, L.; Expert, D.; Barras, F. SoxR-dependent response to oxidative stress and virulence of *Erwinia chrysanthemi*: The key role of SufC, an orphan ABC ATPase. *Mol. Microbiol.* **2001**, *39*, 960–972. [[CrossRef](#)] [[PubMed](#)]
45. Takahashi, Y.; Tokumoto, U. A third bacterial system for the assembly of iron-sulfur clusters with homologs in archaea and plastids. *J. Biol. Chem.* **2002**, *277*, 28380–28383. [[CrossRef](#)] [[PubMed](#)]
46. Nyvltova, E.; Sutak, R.; Harant, K.; Sedinova, M.; Hrdy, I.; Paces, J.; Vlcek, C.; Tachezy, J. NIF-type iron-sulfur cluster assembly system is duplicated and distributed in the mitochondria and cytosol of *Mastigamoeba balamuthi*. *Proc. Natl. Acad. Sci. USA* **2013**, *110*, 7371–7376. [[CrossRef](#)]

47. Garcia, P.S.; Gribaldo, S.; Py, B.; Barras, F. The SUF system: An ABC ATPase-dependent protein complex with a role in Fe–S cluster biogenesis. *Res. Microbiol.* **2019**, *170*, 426–434. [[CrossRef](#)]
48. Freibert, S.A.; Goldberg, A.V.; Hacker, C.; Molik, S.; Dean, P.; Williams, T.A.; Nakjang, S.; Long, S.; Sendra, K.; Bill, E.; et al. Evolutionary conservation and in vitro reconstitution of microsporidian iron-sulfur cluster biosynthesis. *Nat. Commun.* **2017**, *8*, 13932. [[CrossRef](#)]
49. Couturier, J.; Touraine, B.; BRIAT, J.-F.; Gaymard, F.; Rouhier, N. The iron-sulfur cluster assembly machineries in plants: Current knowledge and open questions. *Front. Plant Sci.* **2013**, *4*, 1–22. [[CrossRef](#)]
50. Balk, J.; Schaedler, T.A. Iron Cofactor Assembly in Plants. *Annu. Rev. Plant Biol.* **2014**, *65*, 125–153. [[CrossRef](#)]
51. Dai, Y.; Outten, F.W. The E. coli SufS-SufE sulfur transfer system is more resistant to oxidative stress than IscS-IscU. *FEBS Lett.* **2012**, *586*, 4016–4022. [[CrossRef](#)]
52. Trotter, V.; Vinella, D.; Loiseau, L.; Ollagnier de Choudens, S.; Fontecave, M.; Barras, F. The CsdA cysteine desulphurase promotes Fe/S biogenesis by recruiting Suf components and participates to a new sulphur transfer pathway by recruiting CsdL (ex-YgdL), a ubiquitin-modifying-like protein. *Mol. Microbiol.* **2009**, *74*, 1527–1542. [[CrossRef](#)] [[PubMed](#)]
53. Fosset, C.; Chauveau, M.J.; Guillon, B.; Canal, F.; Drapier, J.C.; Bouton, C. RNA silencing of mitochondrial m-Nfs1 reduces Fe–S enzyme activity both in mitochondria and cytosol of mammalian cells. *J. Biol. Chem.* **2006**, *281*, 25398–25406. [[CrossRef](#)] [[PubMed](#)]
54. Kispal, G.; Csere, P.; Prohl, C.; Lill, R. The mitochondrial proteins Atm1p and Nfs1p are essential for biogenesis of cytosolic Fe/S proteins. *EMBO J.* **1999**, *18*, 3981–3989. [[CrossRef](#)] [[PubMed](#)]
55. Marelja, Z.; Stocklein, W.; Nimtz, M.; Leimkuhler, S. A novel role for human Nfs1 in the cytoplasm: Nfs1 acts as a sulfur donor for MOCS3, a protein involved in molybdenum cofactor biosynthesis. *J. Biol. Chem.* **2008**, *283*, 25178–25185. [[CrossRef](#)]
56. Muhlenhoff, U.; Balk, J.; Richhardt, N.; Kaiser, J.T.; Sipos, K.; Kispal, G.; Lill, R. Functional characterization of the eukaryotic cysteine desulfurase Nfs1p from *Saccharomyces cerevisiae*. *J. Biol. Chem.* **2004**, *279*, 36906–36915. [[CrossRef](#)]
57. Pandey, A.K.; Pain, J.; Dancis, A.; Pain, D. Mitochondria export iron-sulfur and sulfur intermediates to the cytoplasm for iron-sulfur cluster assembly and tRNA thiolation in yeast. *J. Biol. Chem.* **2019**, *294*, 9489–9502. [[CrossRef](#)]
58. Pastore, A.; Puccio, H. Frataxin: A protein in search for a function. *J. Neurochem.* **2013**, *126* (Suppl. S1), 43–52. [[CrossRef](#)]
59. Roche, B.; Huguenot, A.; Barras, F.; Py, B. The iron-binding CyaY and IscX proteins assist the ISC-catalyzed Fe–S biogenesis in *Escherichia coli*. *Mol. Microbiol.* **2015**, *95*, 605–623. [[CrossRef](#)]
60. Van Vranken, J.G.; Nowinski, S.M.; Clowers, K.J.; Jeong, M.Y.; Ouyang, Y.; Berg, J.A.; Gygi, J.P.; Gygi, S.P.; Winge, D.R.; Rutter, J. ACP Acylation Is an Acetyl-CoA-Dependent Modification Required for Electron Transport Chain Assembly. *Mol. Cell* **2018**, *71*, 567–580 e564. [[CrossRef](#)]
61. Agar, J.N.; Krebs, C.; Frazzon, J.; Huynh, B.H.; Dean, D.R.; Johnson, M.K. IscU as a scaffold for iron-sulfur cluster biosynthesis: Sequential assembly of [2Fe–2S] and [4Fe–4S] clusters in IscU. *Biochemistry* **2000**, *39*, 7856–7862. [[CrossRef](#)]
62. Mansy, S.S.; Wu, G.; Surerus, K.K.; Cowan, J.A. Iron-sulfur cluster biosynthesis. *Thermatoga maritima* IscU is a structured iron-sulfur cluster assembly protein. *J. Biol. Chem.* **2002**, *277*, 21397–21404. [[CrossRef](#)] [[PubMed](#)]
63. Raulfs, E.C.; O’Carroll, I.P.; Dos Santos, P.C.; Unciuleac, M.C.; Dean, D.R. In vivo iron-sulfur cluster formation. *Proc. Natl. Acad. Sci. USA* **2008**, *105*, 8591–8596. [[CrossRef](#)]
64. Shimomura, Y.; Wada, K.; Fukuyama, K.; Takahashi, Y. The asymmetric trimeric architecture of [2Fe–2S] IscU: Implications for its scaffolding during iron-sulfur cluster biosynthesis. *J. Mol. Biol.* **2008**, *383*, 133–143. [[CrossRef](#)] [[PubMed](#)]
65. Bonomi, F.; Iametti, S.; Morleo, A.; Ta, D.; Vickery, L.E. Facilitated transfer of IscU-[2Fe2S] clusters by chaperone-mediated ligand exchange. *Biochemistry* **2011**, *50*, 9641–9650. [[CrossRef](#)] [[PubMed](#)]
66. Marinoni, E.N.; de Oliveira, J.S.; Nicolet, Y.; Amara, P.; Dean, D.R.; Fontecilla-Camps, J.C. (IscS-IscU)₂ complex structures provide insights into Fe₂S₂ biogenesis and transfer. *Angew. Chem. Int. Ed. Engl.* **2012**, *51*, 5439–5442. [[CrossRef](#)] [[PubMed](#)]
67. Boniecki, M.T.; Freibert, S.A.; Muhlenhoff, U.; Lill, R.; Cygler, M. Structure and functional dynamics of the mitochondrial Fe/S cluster synthesis complex. *Nat. Commun.* **2017**, *8*, 1287. [[CrossRef](#)]

68. Fox, N.G.; Martelli, A.; Nabhan, J.F.; Janz, J.; Borkowska, O.; Bulawa, C.; Yue, W.W. Zinc(II) binding on human wild-type ISCU and Met140 variants modulates NFS1 desulfurase activity. *Biochimie* **2018**, *152*, 211–218. [[CrossRef](#)]
69. Iannuzzi, C.; Adrover, M.; Puglisi, R.; Yan, R.; Temussi, P.A.; Pastore, A. The role of zinc in the stability of the marginally stable IscU scaffold protein. *Protein Sci.* **2014**, *23*, 1208–1219. [[CrossRef](#)]
70. Kim, J.H.; Fuzery, A.K.; Tonelli, M.; Ta, D.T.; Westler, W.M.; Vickery, L.E.; Markley, J.L. Structure and dynamics of the iron-sulfur cluster assembly scaffold protein IscU and its interaction with the cochaperone HscB. *Biochemistry* **2009**, *48*, 6062–6071. [[CrossRef](#)]
71. Ramelot, T.A.; Cort, J.R.; Goldsmith-Fischman, S.; Kornhaber, G.J.; Xiao, R.; Shastry, R.; Acton, T.B.; Honig, B.; Montelione, G.T.; Kennedy, M.A. Solution NMR structure of the iron-sulfur cluster assembly protein U (IscU) with zinc bound at the active site. *J. Mol. Biol.* **2004**, *344*, 567–583. [[CrossRef](#)]
72. Yan, R.; Kelly, G.; Pastore, A. The scaffold protein IscU retains a structured conformation in the Fe–S cluster assembly complex. *ChemBiochem* **2014**, *15*, 1682–1686. [[CrossRef](#)] [[PubMed](#)]
73. Fox, N.G.; Yu, X.; Feng, X.; Bailey, H.J.; Martelli, A.; Nabhan, J.F.; Strain-Damerell, C.; Bulawa, C.; Yue, W.W.; Han, S. Structure of the human frataxin-bound iron-sulfur cluster assembly complex provides insight into its activation mechanism. *Nat. Commun.* **2019**, *10*, 2210. [[CrossRef](#)]
74. Bertini, I.; Cowan, J.A.; Del Bianco, C.; Luchinat, C.; Mansy, S.S. Thermotoga maritima IscU. Structural characterization and dynamics of a new class of metallochaperone. *J. Mol. Biol.* **2003**, *331*, 907–924. [[CrossRef](#)]
75. Cai, K.; Frederick, R.O.; Kim, J.H.; Reinen, N.M.; Tonelli, M.; Markley, J.L. Human mitochondrial chaperone (mtHSP70) and cysteine desulfurase (NFS1) bind preferentially to the disordered conformation, whereas co-chaperone (HSC20) binds to the structured conformation of the iron-sulfur cluster scaffold protein (ISCU). *J. Biol. Chem.* **2013**, *288*, 28755–28770. [[CrossRef](#)] [[PubMed](#)]
76. Mansy, S.S.; Wu, S.P.; Cowan, J.A. Iron-sulfur cluster biosynthesis: Biochemical characterization of the conformational dynamics of Thermotoga maritima IscU and the relevance for cellular cluster assembly. *J. Biol. Chem.* **2004**, *279*, 10469–10475. [[CrossRef](#)]
77. Kim, J.H.; Tonelli, M.; Markley, J.L. Disordered form of the scaffold protein IscU is the substrate for iron-sulfur cluster assembly on cysteine desulfurase. *Proc. Natl. Acad. Sci. USA* **2012**, *109*, 454–459. [[CrossRef](#)]
78. Lin, C.W.; McCabe, J.W.; Russell, D.H.; Barondeau, D.P. Molecular Mechanism of ISC Iron-Sulfur Cluster Biogenesis Revealed by High-Resolution Native Mass Spectrometry. *J. Am. Chem. Soc.* **2020**, *142*, 6018–6029. [[CrossRef](#)]
79. Lewis, B.E.; Mason, Z.; Rodrigues, A.V.; Nuth, M.; Dizin, E.; Cowan, J.A.; Stemmler, T.L. Unique roles of iron and zinc binding to the yeast Fe–S cluster scaffold assembly protein “Isu1”. *Metallomics* **2019**, *11*, 1820–1835. [[CrossRef](#)]
80. Rodrigues, A.V.; Kandegedara, A.; Rotondo, J.A.; Dancis, A.; Stemmler, T.L. Iron loading site on the Fe–S cluster assembly scaffold protein is distinct from the active site. *Biometals* **2015**, *28*, 567–576. [[CrossRef](#)]
81. Dzul, S.P.; Rocha, A.G.; Rawat, S.; Kandegedara, A.; Kusowski, A.; Pain, J.; Murari, A.; Pain, D.; Dancis, A.; Stemmler, T.L. In vitro characterization of a novel Isu homologue from *Drosophila melanogaster* for de novo FeS-cluster formation. *Metallomics* **2017**, *9*, 48–60. [[CrossRef](#)]
82. Adamec, J.; Rusnak, F.; Owen, W.G.; Naylor, S.; Benson, L.M.; Gacy, A.M.; Isaya, G. Iron-dependent self-assembly of recombinant yeast frataxin: Implications for Friedreich ataxia. *Am. J. Hum. Genet.* **2000**, *67*, 549–562. [[CrossRef](#)] [[PubMed](#)]
83. Cavadini, P.; O’Neill, H.A.; Benada, O.; Isaya, G. Assembly and iron-binding properties of human frataxin, the protein deficient in Friedreich ataxia. *Hum. Mol. Genet.* **2002**, *11*, 217–227. [[CrossRef](#)] [[PubMed](#)]
84. Ding, H.; Yang, J.; Coleman, L.C.; Yeung, S. Distinct iron binding property of two putative iron donors for the iron-sulfur cluster assembly: IscA and the bacterial frataxin ortholog CyaY under physiological and oxidative stress conditions. *J. Biol. Chem.* **2007**, *282*, 7997–8004. [[CrossRef](#)]
85. Gakh, O.; Adamec, J.; Gacy, A.M.; Twesten, R.D.; Owen, W.G.; Isaya, G. Physical evidence that yeast frataxin is an iron storage protein. *Biochemistry* **2002**, *41*, 6798–6804. [[CrossRef](#)] [[PubMed](#)]
86. Layer, G.; Ollagnier-de Choudens, S.; Sanakis, Y.; Fontecave, M. Iron-sulfur cluster biosynthesis: Characterization of Escherichia coli CYaY as an iron donor for the assembly of [2Fe–2S] clusters in the scaffold IscU. *J. Biol. Chem.* **2006**, *281*, 16256–16263. [[CrossRef](#)] [[PubMed](#)]
87. Yoon, T.; Cowan, J.A. Iron-sulfur cluster biosynthesis. Characterization of frataxin as an iron donor for assembly of [2Fe–2S] clusters in ISU-type proteins. *J. Am. Chem. Soc.* **2003**, *125*, 6078–6084. [[CrossRef](#)]

88. Parent, A.; Elduque, X.; Cornu, D.; Belot, L.; Le Caer, J.P.; Grandas, A.; Toledano, M.B.; D'Autreaux, B. Mammalian frataxin directly enhances sulfur transfer of NFS1 persulfide to both ISCU and free thiols. *Nat. Commun.* **2015**, *6*, 5686. [[CrossRef](#)]
89. Patra, S.; Barondeau, D.P. Mechanism of activation of the human cysteine desulfurase complex by frataxin. *Proc. Natl. Acad. Sci. USA* **2019**, *116*, 19421–19430. [[CrossRef](#)]
90. Armas, A.M.; Balparda, M.; Terenzi, A.; Busi, M.V.; Pagani, M.A.; Gomez-Casati, D.F. Ferrochelatase activity of plant frataxin. *Biochimie* **2019**, *156*, 118–122. [[CrossRef](#)]
91. Bellanda, M.; Maso, L.; Doni, D.; Bortolus, M.; De Rosa, E.; Lunardi, F.; Alfonsi, A.; Noguera, M.E.; Herrera, M.G.; Santos, J.; et al. Exploring iron-binding to human frataxin and to selected Friedreich ataxia mutants by means of NMR and EPR spectroscopies. *Biochim. Biophys. Acta Proteins Proteom.* **2019**, *1867*, 140254. [[CrossRef](#)]
92. Cai, K.; Frederick, R.O.; Tonelli, M.; Markley, J.L. Interactions of iron-bound frataxin with ISCU and ferredoxin on the cysteine desulfurase complex leading to Fe–S cluster assembly. *J. Inorg. Biochem.* **2018**, *183*, 107–116. [[CrossRef](#)]
93. Castro, I.H.; Pignataro, M.F.; Sewell, K.E.; Espeche, L.D.; Herrera, M.G.; Noguera, M.E.; Dain, L.; Nadra, A.D.; Aran, M.; Smal, C.; et al. Frataxin Structure and Function. *Subcell Biochem.* **2019**, *93*, 393–438.
94. Gakh, O.; Ranatunga, W.; Galeano, B.K.; Smith, D.S.T.; Thompson, J.R.; Isaya, G. Defining the Architecture of the Core Machinery for the Assembly of Fe–S Clusters in Human Mitochondria. *Methods Enzymol.* **2017**, *595*, 107–160.
95. Galeano, B.K.; Ranatunga, W.; Gakh, O.; Smith, D.Y.; Thompson, J.R.; Isaya, G. Zinc and the iron donor frataxin regulate oligomerization of the scaffold protein to form new Fe–S cluster assembly centers. *Metallomics* **2017**, *9*, 773–801. [[CrossRef](#)]
96. Ranatunga, W.; Gakh, O.; Galeano, B.K.; Smith, D.Y.T.; Soderberg, C.A.; Al-Karadaghi, S.; Thompson, J.R.; Isaya, G. Architecture of the Yeast Mitochondrial Iron-Sulfur Cluster Assembly Machinery: The Sub-Complex Formed by the Iron Donor, Yfh1 Protein, and the Scaffold, Isu1 Protein. *J. Biol. Chem.* **2016**, *291*, 10378–10398. [[CrossRef](#)]
97. Babcock, M.; de Silva, D.; Oaks, R.; Davis-Kaplan, S.; Jiralerspong, S.; Montermini, L.; Pandolfo, M.; Kaplan, J. Regulation of mitochondrial iron accumulation by Yfh1p, a putative homolog of frataxin. *Science* **1997**, *276*, 1709–1712. [[CrossRef](#)] [[PubMed](#)]
98. Duby, G.; Foury, F.; Ramazzotti, A.; Herrmann, J.; Lutz, T. A non-essential function for yeast frataxin in iron-sulfur cluster assembly. *Hum. Mol. Genet.* **2002**, *11*, 2635–2643. [[CrossRef](#)] [[PubMed](#)]
99. Foury, F.; Cazzalini, O. Deletion of the yeast homologue of the human gene associated with Friedreich's ataxia elicits iron accumulation in mitochondria. *FEBS Lett.* **1997**, *411*, 373–377. [[CrossRef](#)]
100. Puccio, H.; Simon, D.; Cossee, M.; Criqui-Filipe, P.; Tiziano, F.; Melki, J.; Hindelang, C.; Matyas, R.; Rustin, P.; Koenig, M. Mouse models for Friedreich ataxia exhibit cardiomyopathy, sensory nerve defect and Fe–S enzyme deficiency followed by intramitochondrial iron deposits. *Nat. Genet.* **2001**, *27*, 181–186. [[CrossRef](#)]
101. Rotig, A.; de Lonlay, P.; Chretien, D.; Foury, F.; Koenig, M.; Sidi, D.; Munnich, A.; Rustin, P. Aconitase and mitochondrial iron-sulphur protein deficiency in Friedreich ataxia. *Nat. Genet.* **1997**, *17*, 215–217. [[CrossRef](#)] [[PubMed](#)]
102. Gerber, J.; Muhlenhoff, U.; Lill, R. An interaction between frataxin and Isu1/Nfs1 that is crucial for Fe/S cluster synthesis on Isu1. *EMBO Rep.* **2003**, *4*, 906–911. [[CrossRef](#)]
103. Ramazzotti, A.; Vanmansart, V.; Foury, F. Mitochondrial functional interactions between frataxin and Isu1p, the iron-sulfur cluster scaffold protein, in *Saccharomyces cerevisiae*. *FEBS Lett.* **2004**, *557*, 215–220. [[CrossRef](#)]
104. Schmucker, S.; Martelli, A.; Colin, F.; Page, A.; Wattenhofer-Donze, M.; Reutenauer, L.; Puccio, H. Mammalian frataxin: An essential function for cellular viability through an interaction with a preformed ISCU/NFS1/ISD11 iron-sulfur assembly complex. *PLoS ONE* **2011**, *6*, e16199. [[CrossRef](#)] [[PubMed](#)]
105. Prischi, F.; Konarev, P.V.; Iannuzzi, C.; Pastore, C.; Adinolfi, S.; Martin, S.R.; Svergun, D.I.; Pastore, A. Structural bases for the interaction of frataxin with the central components of iron-sulphur cluster assembly. *Nat. Commun.* **2010**, *1*, 95. [[CrossRef](#)]
106. Campuzano, V.; Montermini, L.; Molto, M.D.; Pianese, L.; Cossee, M.; Cavalcanti, F.; Monros, E.; Rodius, F.; Duclos, F.; Monticelli, A.; et al. Friedreich's ataxia: Autosomal recessive disease caused by an intronic GAA triplet repeat expansion. *Science* **1996**, *271*, 1423–1427. [[CrossRef](#)] [[PubMed](#)]

107. Sanchez-Casis, G.; Cote, M.; Barbeau, A. Pathology of the heart in Friedreich's ataxia: Review of the literature and report of one case. *Can. J. Neurol. Sci.* **1976**, *3*, 349–354. [[CrossRef](#)]
108. Cook, J.D.; Bencze, K.Z.; Jankovic, A.D.; Crater, A.K.; Busch, C.N.; Bradley, P.B.; Stemmler, A.J.; Spaller, M.R.; Stemmler, T.L. Monomeric yeast frataxin is an iron-binding protein. *Biochemistry* **2006**, *45*, 7767–7777. [[CrossRef](#)]
109. O'Neill, H.A.; Gakh, O.; Isaya, G. Supramolecular assemblies of human frataxin are formed via subunit-subunit interactions mediated by a non-conserved amino-terminal region. *J. Mol. Biol.* **2005**, *345*, 433–439. [[CrossRef](#)]
110. Aloria, K.; Schilke, B.; Andrew, A.; Craig, E.A. Iron-induced oligomerization of yeast frataxin homologue Yfh1 is dispensable in vivo. *EMBO Rep.* **2004**, *5*, 1096–1101. [[CrossRef](#)]
111. Schmucker, S.; Argentini, M.; Carelle-Calmels, N.; Martelli, A.; Puccio, H. The in vivo mitochondrial two-step maturation of human frataxin. *Hum. Mol. Genet.* **2008**, *17*, 3521–3531. [[CrossRef](#)]
112. Seguin, A.; Sutak, R.; Bulteau, A.L.; Garcia-Serres, R.; Oddou, J.L.; Lefevre, S.; Santos, R.; Dancis, A.; Camadro, J.M.; Latour, J.M.; et al. Evidence that yeast frataxin is not an iron storage protein in vivo. *Biochim. Biophys. Acta* **2010**, *1802*, 531–538. [[CrossRef](#)] [[PubMed](#)]
113. Muhlenhoff, U.; Richhardt, N.; Ristow, M.; Kispal, G.; Lill, R. The yeast frataxin homolog Yfh1p plays a specific role in the maturation of cellular Fe/S proteins. *Hum. Mol. Genet.* **2002**, *11*, 2025–2036. [[CrossRef](#)]
114. Stehling, O.; Wilbrecht, C.; Lill, R. Mitochondrial iron-sulfur protein biogenesis and human disease. *Biochimie* **2014**, *100*, 61–77. [[CrossRef](#)] [[PubMed](#)]
115. Adinolfi, S.; Nair, M.; Politou, A.; Bayer, E.; Martin, S.; Temussi, P.; Pastore, A. The factors governing the thermal stability of frataxin orthologues: How to increase a protein's stability. *Biochemistry* **2004**, *43*, 6511–6518. [[CrossRef](#)] [[PubMed](#)]
116. Bou-Abdallah, F.; Adinolfi, S.; Pastore, A.; Laue, T.M.; Dennis Chasteen, N. Iron binding and oxidation kinetics in frataxin CyaY of Escherichia coli. *J. Mol. Biol.* **2004**, *341*, 605–615. [[CrossRef](#)] [[PubMed](#)]
117. Yoon, T.; Dizin, E.; Cowan, J.A. N-terminal iron-mediated self-cleavage of human frataxin: Regulation of iron binding and complex formation with target proteins. *J. Biol. Inorg. Chem.* **2007**, *12*, 535–542. [[CrossRef](#)] [[PubMed](#)]
118. Huang, J.; Dizin, E.; Cowan, J.A. Mapping iron binding sites on human frataxin: Implications for cluster assembly on the ISU Fe–S cluster scaffold protein. *J. Biol. Inorg. Chem.* **2008**, *13*, 825–836. [[CrossRef](#)]
119. Ding, B.; Smith, E.S.; Ding, H. Mobilization of the iron centre in IscA for the iron-sulphur cluster assembly in IscU. *Biochem. J.* **2005**, *389*, 797–802. [[CrossRef](#)]
120. Ding, H.; Clark, R.J.; Ding, B. IscA mediates iron delivery for assembly of iron-sulfur clusters in IscU under the limited accessible free iron conditions. *J. Biol. Chem.* **2004**, *279*, 37499–37504. [[CrossRef](#)]
121. Lu, J.; Bitoun, J.P.; Tan, G.; Wang, W.; Min, W.; Ding, H. Iron-binding activity of human iron-sulfur cluster assembly protein hIscA1. *Biochem. J.* **2010**, *428*, 125–131. [[CrossRef](#)]
122. Lu, J.; Yang, J.; Tan, G.; Ding, H. Complementary roles of SufA and IscA in the biogenesis of iron-sulfur clusters in Escherichia coli. *Biochem. J.* **2008**, *409*, 535–543. [[CrossRef](#)] [[PubMed](#)]
123. Yang, J.; Bitoun, J.P.; Ding, H. Interplay of IscA and IscU in biogenesis of iron-sulfur clusters. *J. Biol. Chem.* **2006**, *281*, 27956–27963. [[CrossRef](#)] [[PubMed](#)]
124. Ding, H.; Clark, R.J. Characterization of iron binding in IscA, an ancient iron-sulphur cluster assembly protein. *Biochem. J.* **2004**, *379*, 433–440. [[CrossRef](#)]
125. Mapolelo, D.T.; Zhang, B.; Naik, S.G.; Huynh, B.H.; Johnson, M.K. Spectroscopic and functional characterization of iron-bound forms of Azotobacter vinelandii (Nif)IscA. *Biochemistry* **2012**, *51*, 8056–8070. [[CrossRef](#)]
126. Gupta, V.; Sendra, M.; Naik, S.G.; Chahal, H.K.; Huynh, B.H.; Outten, F.W.; Fontecave, M.; Ollagnier de Choudens, S. Native Escherichia coli SufA, coexpressed with SufBCDSE, purifies as a [2Fe–2S] protein and acts as an Fe–S transporter to Fe–S target enzymes. *J. Am. Chem. Soc.* **2009**, *131*, 6149–6153. [[CrossRef](#)] [[PubMed](#)]
127. Morimoto, K.; Yamashita, E.; Kondou, Y.; Lee, S.J.; Arisaka, F.; Tsukihara, T.; Nakai, M. The asymmetric IscA homodimer with an exposed [2Fe–2S] cluster suggests the structural basis of the Fe–S cluster biosynthetic scaffold. *J. Mol. Biol.* **2006**, *360*, 117–132. [[CrossRef](#)]

128. Wang, W.; Huang, H.; Tan, G.; Si, F.; Liu, M.; Landry, A.P.; Lu, J.; Ding, H. In vivo evidence for the iron-binding activity of an iron-sulfur cluster assembly protein IscA in *Escherichia coli*. *Biochem. J.* **2010**, *432*, 429–436. [[CrossRef](#)]
129. Zeng, J.; Geng, M.; Jiang, H.; Liu, Y.; Liu, J.; Qiu, G. The IscA from *Acidithiobacillus ferrooxidans* is an iron-sulfur protein which assemble the [Fe₄S₄] cluster with intracellular iron and sulfur. *Arch. Biochem. Biophys.* **2007**, *463*, 237–244. [[CrossRef](#)]
130. Mapolelo, D.T.; Zhang, B.; Randeniya, S.; Albetel, A.N.; Li, H.; Couturier, J.; Outten, C.E.; Rouhier, N.; Johnson, M.K. Monothiol glutaredoxins and A-type proteins: Partners in Fe–S cluster trafficking. *Dalton Trans.* **2013**, *42*, 3107–3115. [[CrossRef](#)] [[PubMed](#)]
131. Kim, K.D.; Chung, W.H.; Kim, H.J.; Lee, K.C.; Roe, J.H. Monothiol glutaredoxin Grx5 interacts with Fe–S scaffold proteins Isa1 and Isa2 and supports Fe–S assembly and DNA integrity in mitochondria of fission yeast. *Biochem. Biophys. Res. Commun.* **2010**, *392*, 467–472. [[CrossRef](#)] [[PubMed](#)]
132. Gelling, C.; Dawes, I.W.; Richhardt, N.; Lill, R.; Muhlenhoff, U. Mitochondrial Iba57p is required for Fe/S cluster formation on aconitase and activation of radical SAM enzymes. *Mol. Cell Biol.* **2008**, *28*, 1851–1861. [[CrossRef](#)]
133. Tokumoto, U.; Nomura, S.; Minami, Y.; Mihara, H.; Kato, S.; Kurihara, T.; Esaki, N.; Kanazawa, H.; Matsubara, H.; Takahashi, Y. Network of protein-protein interactions among iron-sulfur cluster assembly proteins in *Escherichia coli*. *J. Biochem.* **2002**, *131*, 713–719. [[CrossRef](#)] [[PubMed](#)]
134. Al-Karadaghi, S.; Franco, R.; Hansson, M.; Shelnutt, J.A.; Isaya, G.; Ferreira, G.C. Chelatas: Distort to select? *Trends Biochem. Sci.* **2006**, *31*, 135–142. [[CrossRef](#)] [[PubMed](#)]
135. Foster, A.W.; Osman, D.; Robinson, N.J. Metal preferences and metallation. *J. Biol. Chem.* **2014**, *289*, 28095–28103. [[CrossRef](#)]
136. Capdevila, D.A.; Edmonds, K.A.; Giedroc, D.P. Metallochaperones and metalloregulation in bacteria. *Essays Biochem.* **2017**, *61*, 177–200.
137. Philpott, C.C.; Jadhav, S. The ins and outs of iron: Escorting iron through the mammalian cytosol. *Free Radic Biol. Med.* **2019**, *133*, 112–117. [[CrossRef](#)]
138. Kruszewski, M. The role of labile iron pool in cardiovascular diseases. *Acta Biochim. Pol.* **2004**, *51*, 471–480. [[CrossRef](#)]
139. Wofford, J.D.; Bolaji, N.; Dziuba, N.; Outten, F.W.; Lindahl, P.A. Evidence that a respiratory shield in *Escherichia coli* protects a low-molecular-mass Fe(II) pool from O₂-dependent oxidation. *J. Biol. Chem.* **2019**, *294*, 50–62. [[CrossRef](#)]
140. Lindahl, P.A.; Moore, M.J. Labile Low-Molecular-Mass Metal Complexes in Mitochondria: Trials and Tribulations of a Burgeoning Field. *Biochemistry* **2016**, *55*, 4140–4153. [[CrossRef](#)]
141. McCormick, S.P.; Moore, M.J.; Lindahl, P.A. Detection of Labile Low-Molecular-Mass Transition Metal Complexes in Mitochondria. *Biochemistry* **2015**, *54*, 3442–3453. [[CrossRef](#)]
142. Moore, M.J.; Wofford, J.D.; Dancis, A.; Lindahl, P.A. Recovery of mrs3Δmrs4Δ *Saccharomyces cerevisiae* Cells under Iron-Sufficient Conditions and the Role of Fe580. *Biochemistry* **2018**, *57*, 672–683. [[CrossRef](#)] [[PubMed](#)]
143. Hider, R.C.; Kong, X.L. Glutathione: A key component of the cytoplasmic labile iron pool. *Biometals* **2011**, *24*, 1179–1187. [[CrossRef](#)] [[PubMed](#)]
144. Cupp-Vickery, J.R.; Urbina, H.; Vickery, L.E. Crystal structure of IscS, a cysteine desulfurase from *Escherichia coli*. *J. Mol. Biol.* **2003**, *330*, 1049–1059. [[CrossRef](#)]
145. Fujii, T.; Maeda, M.; Mihara, H.; Kurihara, T.; Esaki, N.; Hata, Y. Structure of a NifS homologue: X-ray structure analysis of CsdB, an *Escherichia coli* counterpart of mammalian selenocysteine lyase. *Biochemistry* **2000**, *39*, 1263–1273. [[CrossRef](#)] [[PubMed](#)]
146. Kaiser, J.T.; Clausen, T.; Bourenkow, G.P.; Bartunik, H.D.; Steinbacher, S.; Huber, R. Crystal structure of a NifS-like protein from *Thermotoga maritima*: Implications for iron sulphur cluster assembly. *J. Mol. Biol.* **2000**, *297*, 451–464. [[CrossRef](#)] [[PubMed](#)]
147. Nakamura, R.; Hikita, M.; Ogawa, S.; Takahashi, Y.; Fujishiro, T. Snapshots of PLP-substrate and PLP-product external aldimines as intermediates in two types of cysteine desulfurase enzymes. *FEBS J.* **2020**, *287*, 1138–1154. [[CrossRef](#)]
148. Roret, T.; Pegeot, H.; Couturier, J.; Mulliert, G.; Rouhier, N.; Didierjean, C. X-ray structures of Nfs2, the plastidial cysteine desulfurase from *Arabidopsis thaliana*. *Acta Crystallogr. F Struct. Biol. Commun.* **2014**, *70*, 1180–1185. [[CrossRef](#)]

149. Rybniker, J.; Pojer, F.; Marienhagen, J.; Kolly, G.S.; Chen, J.M.; van Gumpel, E.; Hartmann, P.; Cole, S.T. The cysteine desulfurase IscS of *Mycobacterium tuberculosis* is involved in iron-sulfur cluster biogenesis and oxidative stress defence. *Biochem. J.* **2014**, *459*, 467–478. [[CrossRef](#)]
150. Shi, R.; Proteau, A.; Villarroya, M.; Moukadiri, I.; Zhang, L.; Trempe, J.F.; Matte, A.; Armengod, M.E.; Cygler, M. Structural basis for Fe–S cluster assembly and tRNA thiolation mediated by IscS protein-protein interactions. *PLoS Biol.* **2010**, *8*, e1000354. [[CrossRef](#)]
151. Cory, S.A.; Van Vranken, J.G.; Brignole, E.J.; Patra, S.; Winge, D.R.; Drennan, C.L.; Rutter, J.; Barondeau, D.P. Structure of human Fe–S assembly subcomplex reveals unexpected cysteine desulfurase architecture and acyl-ACP-ISD11 interactions. *Proc. Natl. Acad. Sci. USA* **2017**, *114*, E5325–E5334. [[CrossRef](#)]
152. Turowski, V.R.; Busi, M.V.; Gomez-Casati, D.F. Structural and functional studies of the mitochondrial cysteine desulfurase from *Arabidopsis thaliana*. *Mol. Plant* **2012**, *5*, 1001–1010. [[CrossRef](#)]
153. Herrera, M.G.; Pignataro, M.F.; Noguera, M.E.; Cruz, K.M.; Santos, J. Rescuing the Rescuer: On the Protein Complex between the Human Mitochondrial Acyl Carrier Protein and ISD11. *ACS Chem. Biol.* **2018**, *13*, 1455–1462. [[CrossRef](#)] [[PubMed](#)]
154. Smith, A.D.; Agar, J.N.; Johnson, K.A.; Frazzon, J.; Amster, I.J.; Dean, D.R.; Johnson, M.K. Sulfur transfer from IscS to IscU: The first step in iron-sulfur cluster biosynthesis. *J. Am. Chem. Soc.* **2001**, *123*, 11103–11104. [[CrossRef](#)]
155. Urbina, H.D.; Silberg, J.J.; Hoff, K.G.; Vickery, L.E. Transfer of sulfur from IscS to IscU during Fe/S cluster assembly. *J. Biol. Chem.* **2001**, *276*, 44521–44526. [[CrossRef](#)] [[PubMed](#)]
156. Smith, A.D.; Frazzon, J.; Dean, D.R.; Johnson, M.K. Role of conserved cysteines in mediating sulfur transfer from IscS to IscU. *FEBS Lett.* **2005**, *579*, 5236–5240. [[CrossRef](#)]
157. Nuth, M.; Yoon, T.; Cowan, J.A. Iron-sulfur cluster biosynthesis: Characterization of iron nucleation sites for assembly of the [2Fe–2S]²⁺ cluster core in IscU proteins. *J. Am. Chem. Soc.* **2002**, *124*, 8774–8775. [[CrossRef](#)]
158. Bridwell-Rabb, J.; Fox, N.G.; Tsai, C.L.; Winn, A.M.; Barondeau, D.P. Human frataxin activates Fe–S cluster biosynthesis by facilitating sulfur transfer chemistry. *Biochemistry* **2014**, *53*, 4904–4913. [[CrossRef](#)] [[PubMed](#)]
159. Selbach, B.P.; Chung, A.H.; Scott, A.D.; George, S.J.; Cramer, S.P.; Dos Santos, P.C. Fe–S Cluster Biogenesis in Gram-Positive Bacteria: SufU Is a Zinc-Dependent Sulfur Transfer Protein. *Biochemistry* **2014**, *53*, 152–160. [[CrossRef](#)] [[PubMed](#)]
160. Adinolfi, S.; Iannuzzi, C.; Prischi, F.; Pastore, C.; Iametti, S.; Martin, S.R.; Bonomi, F.; Pastore, A. Bacterial frataxin CyaY is the gatekeeper of iron-sulfur cluster formation catalyzed by IscS. *Nat. Struct. Mol. Biol.* **2009**, *16*, 390–396. [[CrossRef](#)]
161. Nuth, M.; Cowan, J.A. Iron-sulfur cluster biosynthesis: Characterization of IscU-IscS complex formation and a structural model for sulfide delivery to the [2Fe–2S] assembly site. *J. Biol. Inorg. Chem.* **2009**, *14*, 829–839. [[CrossRef](#)]
162. Tsai, C.L.; Barondeau, D.P. Human frataxin is an allosteric switch that activates the Fe–S cluster biosynthetic complex. *Biochemistry* **2010**, *49*, 9132–9139. [[CrossRef](#)] [[PubMed](#)]
163. Bridwell-Rabb, J.; Iannuzzi, C.; Pastore, A.; Barondeau, D.P. Effector role reversal during evolution: The case of frataxin in Fe–S cluster biosynthesis. *Biochemistry* **2012**, *51*, 2506–2514. [[CrossRef](#)] [[PubMed](#)]
164. Colin, F.; Martelli, A.; Clemancey, M.; Latour, J.M.; Gambarelli, S.; Zepieri, L.; Birck, C.; Page, A.; Puccio, H.; Ollagnier de Choudens, S. Mammalian frataxin controls sulfur production and iron entry during de novo Fe₄S₄ cluster assembly. *J. Am. Chem. Soc.* **2013**, *135*, 733–740. [[CrossRef](#)] [[PubMed](#)]
165. Unciuleac, M.C.; Chandramouli, K.; Naik, S.; Mayer, S.; Huynh, B.H.; Johnson, M.K.; Dean, D.R. In vitro activation of apo-aconitase using a [4Fe–4S] cluster-loaded form of the IscU [Fe–S] cluster scaffolding protein. *Biochemistry* **2007**, *46*, 6812–6821. [[CrossRef](#)]
166. Iannuzzi, C.; Adinolfi, S.; Howes, B.D.; Garcia-Serres, R.; Clemancey, M.; Latour, J.M.; Smulevich, G.; Pastore, A. The role of CyaY in iron sulfur cluster assembly on the *E. coli* IscU scaffold protein. *PLoS ONE* **2011**, *6*, e21992. [[CrossRef](#)]
167. Fox, N.G.; Chakrabarti, M.; McCormick, S.P.; Lindahl, P.A.; Barondeau, D.P. The Human Iron-Sulfur Assembly Complex Catalyzes the Synthesis of [2Fe–2S] Clusters on ISCU2 That Can Be Transferred to Acceptor Molecules. *Biochemistry* **2015**, *54*, 3871–3879. [[CrossRef](#)]
168. Tokumoto, U.; Takahashi, Y. Genetic analysis of the *isc* operon in *Escherichia coli* involved in the biogenesis of cellular iron-sulfur proteins. *J. Biochem.* **2001**, *130*, 63–71. [[CrossRef](#)]

169. Lange, H.; Kaut, A.; Kispal, G.; Lill, R. A mitochondrial ferredoxin is essential for biogenesis of cellular iron-sulfur proteins. *Proc. Natl. Acad. Sci. USA* **2000**, *97*, 1050–1055. [[CrossRef](#)]
170. Djaman, O.; Outten, F.W.; Imlay, J.A. Repair of oxidized iron-sulfur clusters in *Escherichia coli*. *J. Biol. Chem.* **2004**, *279*, 44590–44599. [[CrossRef](#)]
171. Muhlenhoff, U.; Gerber, J.; Richhardt, N.; Lill, R. Components involved in assembly and dislocation of iron-sulfur clusters on the scaffold protein Isu1p. *EMBO J.* **2003**, *22*, 4815–4825. [[CrossRef](#)]
172. Sheftel, A.D.; Stehling, O.; Pierik, A.J.; Elsasser, H.P.; Muhlenhoff, U.; Webert, H.; Hobler, A.; Hannemann, F.; Bernhardt, R.; Lill, R. Humans possess two mitochondrial ferredoxins, Fdx1 and Fdx2, with distinct roles in steroidogenesis, heme, and Fe/S cluster biosynthesis. *Proc. Natl. Acad. Sci. USA* **2010**, *107*, 11775–11780. [[CrossRef](#)] [[PubMed](#)]
173. Shi, Y.; Ghosh, M.; Kovtunovych, G.; Crooks, D.R.; Rouault, T.A. Both human ferredoxins 1 and 2 and ferredoxin reductase are important for iron-sulfur cluster biogenesis. *Biochim. Biophys. Acta* **2012**, *1823*, 484–492. [[CrossRef](#)] [[PubMed](#)]
174. Li, J.; Saxena, S.; Pain, D.; Dancis, A. Adrenodoxin reductase homolog (Arh1p) of yeast mitochondria required for iron homeostasis. *J. Biol. Chem.* **2001**, *276*, 1503–1509. [[CrossRef](#)]
175. Wan, J.T.; Jarrett, J.T. Electron acceptor specificity of ferredoxin (flavodoxin): NADP⁺ oxidoreductase from *Escherichia coli*. *Arch. Biochem. Biophys.* **2002**, *406*, 116–126. [[CrossRef](#)]
176. Yan, R.; Adinolfi, S.; Pastore, A. Ferredoxin, in conjunction with NADPH and ferredoxin-NADP reductase, transfers electrons to the IscS/IscU complex to promote iron-sulfur cluster assembly. *Biochim. Biophys. Acta* **2015**, *1854*, 1113–1117. [[CrossRef](#)]
177. Cai, K.; Tonelli, M.; Frederick, R.O.; Markley, J.L. Human Mitochondrial Ferredoxin 1 (FDX1) and Ferredoxin 2 (FDX2) Both Bind Cysteine Desulfurase and Donate Electrons for Iron-Sulfur Cluster Biosynthesis. *Biochemistry* **2017**, *56*, 487–499. [[CrossRef](#)]
178. Kim, J.H.; Frederick, R.O.; Reinen, N.M.; Troupis, A.T.; Markley, J.L. [2Fe–2S]-ferredoxin binds directly to cysteine desulfurase and supplies an electron for iron-sulfur cluster assembly but is displaced by the scaffold protein or bacterial frataxin. *J. Am. Chem. Soc.* **2013**, *135*, 8117–8120. [[CrossRef](#)]
179. Yan, R.; Konarev, P.V.; Iannuzzi, C.; Adinolfi, S.; Roche, B.; Kelly, G.; Simon, L.; Martin, S.R.; Py, B.; Barras, F.; et al. Ferredoxin competes with bacterial frataxin in binding to the desulfurase IscS. *J. Biol. Chem.* **2013**, *288*, 24777–24787. [[CrossRef](#)]
180. Galardon, E.; Roger, T.; Deschamps, P.; Roussel, P.; Tomas, A.; Artaud, I. Synthesis of a Fe(II)SH complex stabilized by an intramolecular N–H...S hydrogen bond, which acts as a H₂S donor. *Inorg. Chem.* **2012**, *51*, 10068–10070. [[CrossRef](#)]
181. Tsou, C.C.; Chiu, W.C.; Ke, C.H.; Tsai, J.C.; Wang, Y.M.; Chiang, M.H.; Liaw, W.F. Iron(III) bound by hydrosulfide anion ligands: NO-promoted stabilization of the [Fe(III)–SH] motif. *J. Am. Chem. Soc.* **2014**, *136*, 9424–9433. [[CrossRef](#)]
182. Dey, A.; Hocking, R.K.; Larsen, P.; Borovik, A.S.; Hodgson, K.O.; Hedman, B.; Solomon, E.I. X-ray absorption spectroscopy and density functional theory studies of [(H₃buea)Fe^{III}–X]^{n–} (X = S^{2–}, O^{2–}, OH[–]): Comparison of bonding and hydrogen bonding in oxo and sulfido complexes. *J. Am. Chem. Soc.* **2006**, *128*, 9825–9833. [[CrossRef](#)] [[PubMed](#)]
183. Conradie, J.; Tangen, E.; Ghosh, A. Trigonal bipyramidal iron(III) and manganese(III) oxo, sulfido, and selenido complexes. An electronic-structural overview. *J. Inorg. Biochem.* **2006**, *100*, 707–715. [[CrossRef](#)] [[PubMed](#)]
184. Larsen, P.L.; Gupta, R.; Powell, D.R.; Borovik, A.S. Chalcogens as terminal ligands to iron: Synthesis and structure of complexes with Fe(III)–S and Fe(III)–Se motifs. *J. Am. Chem. Soc.* **2004**, *126*, 6522–6523. [[CrossRef](#)] [[PubMed](#)]
185. Li, H.; Outten, C.E. Monothiol CGFS glutaredoxins and BolA-like proteins: [2Fe–2S] binding partners in iron homeostasis. *Biochemistry* **2012**, *51*, 4377–4389. [[CrossRef](#)]
186. Rouhier, N.; Couturier, J.; Johnson, M.K.; Jacquot, J.P. Glutaredoxins: Roles in iron homeostasis. *Trends Biochem. Sci.* **2010**, *35*, 43–52. [[CrossRef](#)]
187. Banci, L.; Brancaccio, D.; Ciofi-Baffoni, S.; Del Conte, R.; Gadepalli, R.; Mikolajczyk, M.; Neri, S.; Piccioli, M.; Winkelman, J. [2Fe–2S] cluster transfer in iron-sulfur protein biogenesis. *Proc. Natl. Acad. Sci. USA* **2014**, *111*, 6203–6208. [[CrossRef](#)]

188. Shakamuri, P.; Zhang, B.; Johnson, M.K. Monothiol glutaredoxins function in storing and transporting [Fe₂S₂] clusters assembled on IscU scaffold proteins. *J. Am. Chem. Soc.* **2012**, *134*, 15213–15216. [[CrossRef](#)]
189. Agar, J.N.; Zheng, L.; Cash, V.L.; Dean, D.R.; Johnson, M.K. Role of the IscU Protein in Iron–Sulfur Cluster Biosynthesis: IscS-mediated Assembly of a [Fe₂S₂] Cluster in IscU. *J. Am. Chem. Soc.* **2000**, *122*, 2136–2137. [[CrossRef](#)]
190. Wu, G.; Mansy, S.S.; Wu Sp, S.P.; Surerus, K.K.; Foster, M.W.; Cowan, J.A. Characterization of an iron-sulfur cluster assembly protein (ISU1) from *Schizosaccharomyces pombe*. *Biochemistry* **2002**, *41*, 5024–5032. [[CrossRef](#)]
191. Tsai, C.L.; Bridwell-Rabb, J.; Barondeau, D.P. Friedreich's ataxia variants I154F and W155R diminish frataxin-based activation of the iron-sulfur cluster assembly complex. *Biochemistry* **2011**, *50*, 6478–6487. [[CrossRef](#)]
192. Bridwell-Rabb, J.; Winn, A.M.; Barondeau, D.P. Structure-function analysis of Friedreich's ataxia mutants reveals determinants of frataxin binding and activation of the Fe–S assembly complex. *Biochemistry* **2011**, *50*, 7265–7274. [[CrossRef](#)] [[PubMed](#)]
193. Fox, N.G.; Das, D.; Chakrabarti, M.; Lindahl, P.A.; Barondeau, D.P. Frataxin Accelerates [2Fe–2S] Cluster Formation on the Human Fe–S Assembly Complex. *Biochemistry* **2015**, *54*, 3880–3889. [[CrossRef](#)] [[PubMed](#)]
194. Pandey, A.; Gordon, D.M.; Pain, J.; Stemmler, T.L.; Dancis, A.; Pain, D. Frataxin directly stimulates mitochondrial cysteine desulfurase by exposing substrate-binding sites, and a mutant Fe–S cluster scaffold protein with frataxin-bypassing ability acts similarly. *J. Biol. Chem.* **2013**, *288*, 36773–36786. [[CrossRef](#)] [[PubMed](#)]
195. Behshad, E.; Parkin, S.E.; Bollinger, J.M., Jr. Mechanism of cysteine desulfurase Slr0387 from *Synechocystis* sp. PCC 6803: Kinetic analysis of cleavage of the persulfide intermediate by chemical reductants. *Biochemistry* **2004**, *43*, 12220–12226. [[CrossRef](#)]
196. Lacourciere, G.M.; Stadtman, T.C. The NIFS protein can function as a selenide delivery protein in the biosynthesis of selenophosphate. *J. Biol. Chem.* **1998**, *273*, 30921–30926. [[CrossRef](#)]
197. Zheng, L.; White, R.H.; Cash, V.L.; Dean, D.R. Mechanism for the desulfurization of L-cysteine catalyzed by the nifS gene product. *Biochemistry* **1994**, *33*, 4714–4720. [[CrossRef](#)]
198. Ponsoero, A.J.; Igbaria, A.; Darch, M.A.; Miled, S.; Outten, C.E.; Winther, J.R.; Palais, G.; D'Autreaux, B.; Delaunay-Moisan, A.; Toledano, M.B. Endoplasmic Reticulum Transport of Glutathione by Sec61 Is Regulated by Ero1 and Bip. *Mol. Cell* **2017**, *67*, 962–973 e965. [[CrossRef](#)]
199. Furne, J.; Saeed, A.; Levitt, M.D. Whole tissue hydrogen sulfide concentrations are orders of magnitude lower than presently accepted values. *Am. J. Physiol. Regul. Integr. Comp. Physiol.* **2008**, *295*, R1479–R1485. [[CrossRef](#)]
200. Ross-Inta, C.; Tsai, C.Y.; Giulivi, C. The mitochondrial pool of free amino acids reflects the composition of mitochondrial DNA-encoded proteins: Indication of a post-translational quality control for protein synthesis. *Biosci. Rep.* **2008**, *28*, 239–249. [[CrossRef](#)]
201. Agar, J.N.; Yuvaniyama, P.; Jack, R.F.; Cash, V.L.; Smith, A.D.; Dean, D.R.; Johnson, M.K. Modular organization and identification of a mononuclear iron-binding site within the NifU protein. *J. Biol. Inorg. Chem.* **2000**, *5*, 167–177. [[CrossRef](#)]
202. Yuvaniyama, P.; Agar, J.N.; Cash, V.L.; Johnson, M.K.; Dean, D.R. NifS-directed assembly of a transient [2Fe–2S] cluster within the NifU protein. *Proc. Natl. Acad. Sci. USA* **2000**, *97*, 599–604. [[CrossRef](#)] [[PubMed](#)]
203. Chandramouli, K.; Unciuleac, M.C.; Naik, S.; Dean, D.R.; Huynh, B.H.; Johnson, M.K. Formation and properties of [4Fe–4S] clusters on the IscU scaffold protein. *Biochemistry* **2007**, *46*, 6804–6811. [[CrossRef](#)] [[PubMed](#)]
204. Outten, F.W. Recent advances in the Suf Fe–S cluster biogenesis pathway: Beyond the Proteobacteria. *Biochim. Biophys. Acta* **2015**, *1853*, 1464–1469. [[CrossRef](#)] [[PubMed](#)]
205. Wollers, S.; Layer, G.; Garcia-Serres, R.; Signor, L.; Clemancey, M.; Latour, J.M.; Fontecave, M.; Ollagnier de Choudens, S. Iron–sulfur (Fe–S) cluster assembly: The SufBC₂D complex is a new type of Fe–S scaffold with a flavin redox cofactor. *J. Biol. Chem.* **2010**, *285*, 23331–23341. [[CrossRef](#)] [[PubMed](#)]
206. Hirabayashi, K.; Yuda, E.; Tanaka, N.; Katayama, S.; Iwasaki, K.; Matsumoto, T.; Kurisu, G.; Outten, F.W.; Fukuyama, K.; Takahashi, Y.; et al. Functional Dynamics Revealed by the Structure of the SufBC₂D Complex, a Novel ATP-binding Cassette (ABC) Protein That Serves as a Scaffold for Iron-Sulfur Cluster Biogenesis. *J. Biol. Chem.* **2015**, *290*, 29717–29731. [[CrossRef](#)] [[PubMed](#)]

207. Riboldi, G.P.; Verli, H.; Frazzon, J. Structural studies of the Enterococcus faecalis SufU [Fe-S] cluster protein. *BMC Biochem.* **2009**, *10*, 3. [[CrossRef](#)]
208. Selbach, B.; Earles, E.; Dos Santos, P.C. Kinetic analysis of the bisubstrate cysteine desulfurase SufS from *Bacillus subtilis*. *Biochemistry* **2010**, *49*, 8794–8802. [[CrossRef](#)] [[PubMed](#)]
209. Albrecht, A.G.; Netz, D.J.; Miethke, M.; Pierik, A.J.; Burghaus, O.; Peuckert, F.; Lill, R.; Marahiel, M.A. SufU is an essential iron-sulfur cluster scaffold protein in *Bacillus subtilis*. *J. Bacteriol.* **2010**, *192*, 1643–1651. [[CrossRef](#)]
210. Yokoyama, N.; Nonaka, C.; Ohashi, Y.; Shioda, M.; Terahata, T.; Chen, W.; Sakamoto, K.; Maruyama, C.; Saito, T.; Yuda, E.; et al. Distinct roles for U-type proteins in iron-sulfur cluster biosynthesis revealed by genetic analysis of the *Bacillus subtilis* sufCDSUB operon. *Mol. Microbiol.* **2018**, *107*, 688–703. [[CrossRef](#)]
211. Saini, A.; Mapolelo, D.T.; Chahal, H.K.; Johnson, M.K.; Outten, F.W. SufD and SufC ATPase activity are required for iron acquisition during in vivo Fe–S cluster formation on SufB. *Biochemistry* **2010**, *49*, 9402–9412. [[CrossRef](#)]
212. Nachin, L.; Loiseau, L.; Expert, D.; Barras, F. SufC: An unorthodox cytoplasmic ABC/ATPase required for [Fe-S] biogenesis under oxidative stress. *EMBO J.* **2003**, *22*, 427–437. [[CrossRef](#)] [[PubMed](#)]
213. Tirupati, B.; Vey, J.L.; Drennan, C.L.; Bollinger, J.M., Jr. Kinetic and structural characterization of Slr0077/SufS, the essential cysteine desulfurase from *Synechocystis* sp. PCC 6803. *Biochemistry* **2004**, *43*, 12210–12219. [[CrossRef](#)] [[PubMed](#)]
214. Outten, F.W.; Wood, M.J.; Munoz, F.M.; Storz, G. The SufE protein and the SufBC₂D complex enhance SufS cysteine desulfurase activity as part of a sulfur transfer pathway for Fe–S cluster assembly in *Escherichia coli*. *J. Biol. Chem.* **2003**, *278*, 45713–45719. [[CrossRef](#)] [[PubMed](#)]
215. Zafrilla, B.; Martinez-Espinosa, R.M.; Esclapez, J.; Perez-Pomares, F.; Bonete, M.J. SufS protein from *Haloferax volcanii* involved in Fe–S cluster assembly in haloarchaea. *Biochim. Biophys. Acta* **2010**, *1804*, 1476–1482. [[CrossRef](#)]
216. Ollagnier-de-Choudens, S.; Lascoux, D.; Loiseau, L.; Barras, F.; Forest, E.; Fontecave, M. Mechanistic studies of the SufS-SufE cysteine desulfurase: Evidence for sulfur transfer from SufS to SufE. *FEBS Lett.* **2003**, *555*, 263–267. [[CrossRef](#)]
217. Singh, H.; Dai, Y.; Outten, F.W.; Busenlehner, L.S. *Escherichia coli* SufE sulfur transfer protein modulates the SufS cysteine desulfurase through allosteric conformational dynamics. *J. Biol. Chem.* **2013**, *288*, 36189–36200. [[CrossRef](#)]
218. Dai, Y.; Kim, D.; Dong, G.; Busenlehner, L.S.; Frantom, P.A.; Outten, F.W. SufE D74R Substitution Alters Active Site Loop Dynamics To Further Enhance SufE Interaction with the SufS Cysteine Desulfurase. *Biochemistry* **2015**, *54*, 4824–4833. [[CrossRef](#)]
219. Kim, D.; Singh, H.; Dai, Y.; Dong, G.; Busenlehner, L.S.; Outten, F.W.; Frantom, P.A. Changes in Protein Dynamics in *Escherichia coli* SufS Reveal a Possible Conserved Regulatory Mechanism in Type II Cysteine Desulfurase Systems. *Biochemistry* **2018**, *57*, 5210–5217. [[CrossRef](#)]
220. Dunkle, J.A.; Bruno, M.R.; Outten, F.W.; Frantom, P.A. Structural Evidence for Dimer-Interface-Driven Regulation of the Type II Cysteine Desulfurase, SufS. *Biochemistry* **2019**, *58*, 687–696. [[CrossRef](#)]
221. Blahut, M.; Wise, C.E.; Bruno, M.R.; Dong, G.; Makris, T.M.; Frantom, P.A.; Dunkle, J.A.; Outten, F.W. Direct observation of intermediates in the SufS cysteine desulfurase reaction reveals functional roles of conserved active-site residues. *J. Biol. Chem.* **2019**, *294*, 12444–12458. [[CrossRef](#)]
222. Kim, S.; Park, S. Structural changes during cysteine desulfurase CsdA and sulfur acceptor CsdE interactions provide insight into the trans-persulfuration. *J. Biol. Chem.* **2013**, *288*, 27172–27180. [[CrossRef](#)] [[PubMed](#)]
223. Dunkle, J.A.; Bruno, M.R.; Frantom, P.A. Structural evidence for a latch mechanism regulating access to the active site of SufS-family cysteine desulfurases. *Acta Crystallogr. D Struct. Biol.* **2020**, *76*, 291–301. [[CrossRef](#)] [[PubMed](#)]
224. Fernández, F.J.; Ardá, A.; López-Esteva, M.; Aranda, J.; Peña-Soler, E.; Garces, F.; Round, A.; Campos-Olivas, R.; Bruix, M.; Coll, M.; et al. Mechanism of Sulfur Transfer Across Protein–Protein Interfaces: The Cysteine Desulfurase Model System. *ACS Catal.* **2016**, *6*, 3975–3984. [[CrossRef](#)]
225. Goldsmith-Fischman, S.; Kuzin, A.; Edstrom, W.C.; Benach, J.; Shastry, R.; Xiao, R.; Acton, T.B.; Honig, B.; Montelione, G.T.; Hunt, J.F. The SufE sulfur-acceptor protein contains a conserved core structure that mediates interdomain interactions in a variety of redox protein complexes. *J. Mol. Biol.* **2004**, *344*, 549–565. [[CrossRef](#)]

226. Liu, G.; Li, Z.; Chiang, Y.; Acton, T.; Montelione, G.T.; Murray, D.; Szyperski, T. High-quality homology models derived from NMR and X-ray structures of *E. coli* proteins YgdK and Suf E suggest that all members of the YgdK/Suf E protein family are enhancers of cysteine desulfurases. *Protein Sci.* **2005**, *14*, 1597–1608. [[CrossRef](#)]
227. Selbach, B.P.; Pradhan, P.K.; Dos Santos, P.C. Protected sulfur transfer reactions by the *Escherichia coli* Suf system. *Biochemistry* **2013**, *52*, 4089–4096. [[CrossRef](#)]
228. Riboldi, G.P.; de Oliveira, J.S.; Frazzon, J. Enterococcus faecalis SufU scaffold protein enhances SufS desulfurase activity by acquiring sulfur from its cysteine-153. *Biochim. Biophys. Acta* **2011**, *1814*, 1910–1918. [[CrossRef](#)]
229. Albrecht, A.G.; Peuckert, F.; Landmann, H.; Miethke, M.; Seubert, A.; Marahiel, M.A. Mechanistic characterization of sulfur transfer from cysteine desulfurase SufS to the iron-sulfur scaffold SufU in *Bacillus subtilis*. *FEBS Lett.* **2011**, *585*, 465–470. [[CrossRef](#)]
230. Kornhaber, G.J.; Snyder, D.; Moseley, H.N.; Montelione, G.T. Identification of zinc-ligated cysteine residues based on ¹³C_{alpha} and ¹³C_{beta} chemical shift data. *J. Biomol. NMR* **2006**, *34*, 259–269. [[CrossRef](#)]
231. Liu, J.; Oganessian, N.; Shin, D.H.; Jancarik, J.; Yokota, H.; Kim, R.; Kim, S.H. Structural characterization of an iron-sulfur cluster assembly protein IscU in a zinc-bound form. *Proteins* **2005**, *59*, 875–881. [[CrossRef](#)]
232. Fujishiro, T.; Terahata, T.; Kunichika, K.; Yokoyama, N.; Maruyama, C.; Asai, K.; Takahashi, Y. Zinc-Ligand Swapping Mediated Complex Formation and Sulfur Transfer between SufS and SufU for Iron-Sulfur Cluster Biogenesis in *Bacillus subtilis*. *J. Am. Chem. Soc.* **2017**, *139*, 18464–18467. [[CrossRef](#)] [[PubMed](#)]
233. Blauenburg, B.; Mielcarek, A.; Altegoer, F.; Fage, C.D.; Linne, U.; Bange, G.; Marahiel, M.A. Crystal Structure of *Bacillus subtilis* Cysteine Desulfurase SufS and Its Dynamic Interaction with Frataxin and Scaffold Protein SufU. *PLoS ONE* **2016**, *11*, e0158749. [[CrossRef](#)] [[PubMed](#)]
234. Yuda, E.; Tanaka, N.; Fujishiro, T.; Yokoyama, N.; Hirabayashi, K.; Fukuyama, K.; Wada, K.; Takahashi, Y. Mapping the key residues of SufB and SufD essential for biosynthesis of iron-sulfur clusters. *Sci. Rep.* **2017**, *7*, 9387. [[CrossRef](#)] [[PubMed](#)]



© 2020 by the authors. Licensee MDPI, Basel, Switzerland. This article is an open access article distributed under the terms and conditions of the Creative Commons Attribution (CC BY) license (<http://creativecommons.org/licenses/by/4.0/>).